Morphology of Model A/B/(C-*block*-D) Ternary Blends and Compatibilization of Two Immiscible Homopolymers A and B with a C-*block*-D Copolymer

Seung Bum Chun and Chang Dae Han*

Department of Polymer Engineering, The University of Akron, Akron, Ohio 44325

Received November 5, 1999; Revised Manuscript Received March 7, 2000

ABSTRACT: The morphology of A/B/(C-*block*-D) ternary blends was investigated by transmission electron microscopy (TEM), and its implications in the compatibilization of two immiscible homopolymers A and B with a C-*block*-D copolymer are discussed. Emphasis is placed on the thermodynamic requirements and the role of order−disorder transition temperature (T_{ODT}) of block copolymer for compatibilization. For the investigation, the following model ternary blends were prepared: (i) 63/27/10 PS/PB/(PαMS-*block*-PI) with PS denoting polystyrene, PB denoting polybutadiene, PαMS denoting poly(α-methylstyrene), and PI denoting polyisoprene; (ii) 63/27/10 PPO/PP/(PS-*block*-PEB) with PPO denoting poly(phenylene oxide), PP denoting polypropylene, and PEB denoting poly(ethylene-*co*-1-butene); and (iii) 63/27/10 PMMA/PP/(PαMS-*block*-PI) with PMMA denoting poly(methyl methacrylate). Blend specimens were prepared by melt blending in a Mini-Max mixer at temperatures above and below the T_{ODT} of block copolymer. The TEM images of ternary blends showed a uniform distribution of (i) PαMS-*block*-PI layer on the surface of PB droplets dispersed in the PS matrix and (ii) PS-*block*-PEB layer on the surface of PP droplets dispersed in the PPO matrix *only when* melt blending was carried out at a temperature above the T_{ODT} of block copolymer. The formation of a uniform interphase between two immiscible homopolymers is attributed to the attractive thermodynamic interactions existing (i) between homopolymer PB and PI block in the 63/27/10 PS/PB/(PαMS-*block*-PI) ternary blend and (ii) between homopolymer PPO and PS block and between homopolymer PP and PEB block in the 63/27/10 PPO/PP/(PS-*block*-PEB) ternary blend. The present study indicates that the T_{ODT} of block copolymer, in relation to melt blending temperature, determines whether the block copolymer can play the role of an effective compatibilizing agent even when thermodynamic requirements (attractive interactions) for compatibilization are satisfied. Thus, we have concluded that attractive thermodynamic interactions alone are not sufficient for compatibilization of two immiscible homopolymers *unless* the T_{ODT} of block copolymer is lower than melt blending temperature, because the viscosity of block copolymer in an ordered state (at $T < T_{ODT}$) is a few orders of magnitude higher than that in the disordered state (at $T > T_{ODT}$). That is, the mobility of block copolymer plays an important role in the compatibilization of two immiscible homopolymers.

Introduction

Compatibilization of two immiscible homopolymers is of fundamental and technological importance, and thus numerous research groups have dealt with this subject. Basically there are two methods to compatibilize two immiscible homopolymers or random copolymers. One method of compatibilization is to use a nonreactive third polymer C which has chemical affinity with two immiscible homopolymers, say A and B, to be melt blended. Since it is very difficult to find or synthesize such a polymer, many research groups turned to block copolymers; namely A-*block*-B copolymers,[1,2] A-*block*-D copolymers,[2,3] A-*block*-D-*block*-A copolymers,[4] or C-*block*-D copolymers.[5−12] Another method of compatibilization is to introduce functional groups into two homopolymers A and B to be melt blended and then use a third polymer C (e.g., graft copolymers) which also has functional groups, so that chemical reactions would take place, during melt blending, between polymers A and C and between polymers B and C. Such compatibilization is often referred to as reactive compatibilization. There are too many papers to cite them all here. The readers are referred to some most recent papers[13−17] and references therein. Understandably, the introduction of functional groups into two existing homopolymers is not a trivial matter, and also finding or synthesizing a graft copolymer C with required functional groups that can react with two functionalized immiscible homopolymers A and B is not a trivial matter either.

Restricting our attention to the use of block copolymer for compatibilizing two immiscible homopolymers, an effective compatibilizing agent is expected to form an "interphase" between two homopolymers, thus significantly improving mechanical properties or adhesion. The formation of an interphase must meet with certain thermodynamic requirements. To produce a mechanically stable interphase between two immiscible homopolymers in the presence of a block copolymer, the block copolymer must be designed, such that each block has a preferential affinity with one of the two homopolymers being melt blended, i.e., the block copolymer must segregate preferentially to the interface between the two immiscible homopolymers.

Figure 1 gives a schematic diagram depicting the thermodynamic requirements for the compatibilization of a pair of immiscible homopolymers A and B with a C-*block*-D copolymer. In Figure 1 we have assumed that homopolymer A and block C, and homopolymer B and block D, respectively, have attractive thermodynamic interactions (i.e., negative interaction parameters: $\chi_{AC} < 0$ and $\chi_{BD} < 0$) and homopolymer A and block D, and homopolymer B and block C, respectively, have repulsive thermodynamic interactions (i.e., $\chi_{AB} > 0$, $\chi_{AD} > 0$, $\chi_{BD} > 0$, and $\chi_{CD} > 0$), where χ_{ij} is the Flory−Huggins interaction parameter. It is our view that a

10.1021/ma9918708 CCC: $19.00
Published on Web 04/12/2000

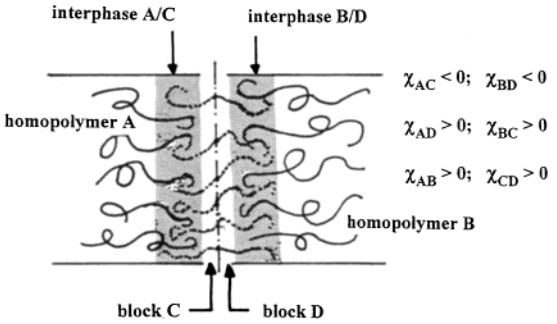

Figure 1. Schematic diagram describing the formation of an interphase between two immiscible homopolymers A and B in the presence of a block copolymer C-*block*-D, where attractive interactions are assumed between homopolymer A and block C and between homopolymer B and block D.

C-*block*-D copolymer can function as an effective compatibilizing agent *only when* an interphase having sufficient thickness is formed, during melt blending, between homopolymer A and block C and between homopolymer B and block D, such that the interphase formed can withstand the external force applied to the ternary blend. In recent years some effort[18−21] has been spent on investigating the homopolymer/block copolymer interface (e.g., segregation of block copolymer to interfaces between immiscible homopolymers) in A/B/(A-*block*-B) ternary blends by various experimental techniques. Other research groups[22,23] investigated adhesion of immiscible polymer interface in the presence of a block copolymer in A/B/(A-*block*-B) ternary blends.

Some theoretical attempts have been made to provide a better understanding of A/B/(A-*block*-B) ternary blends[24−27] and A/B/(C-*block*-D) ternary blends.[28] It should be mentioned that a theoretical approach to the compatibilization of two immiscible homopolymers with a C-*block*-D copolymer must include 11 independent variables: (i) six pairs of the interaction parameters (χ_{AB}, χ_{AC}, χ_{AD}, χ_{BC}, χ_{BD}, and χ_{CD}), (ii) the block lengths of the diblock copolymer (two variables), (iii) the molecular weight of the two homopolymers (two variables), and (iv) the volume fraction of the blend (one variable). The most difficult task for testing a theory, once developed, is to determine all six interaction parameters as a function of temperature. Such information is scarcely available in the literature. It is fair to state that at present a general theory does not exist, which can predict the thickness of the interphase and the distributions of component polymers in the interphase as functions of the 11 independent variables in A/B/(C-*block*-D) ternary blends.

In a recent paper[29] we have pointed out that even when a block copolymer and two homopolymers meet with the necessary thermodynamic requirements (attractive thermodynamic interactions) for compatibilization, the block copolymer would not function as an effective compatibilizing agent *unless* the order−disorder transition temperature (T_{ODT}) of block copolymer is lower than the melt blending temperature. In that study we investigated the morphology of A/B/(A-*block*-B) and A/B/(A-*block*-D) model ternary blends and discussed the compatibilization of two immiscible homopolymers A and B with an A-*block*-B or A-*block*-D copolymer. In doing so, we needed only one interaction parameter, χ_{AB}, to interpret the experimental results for A/B/(A-*block*-B) ternary blends and three interaction parameters, χ_{AB}, χ_{AD}, and χ_{BD}, to interpret the experimental results for A/B/(A-*block*-D) ternary blends.

Very recently, we investigated the morphology of A/B/(C-*block*-D) model ternary blends and compatibilization of two immiscible homopolymers A and B with a C-*block*-D copolymer. For the investigation we first synthesized a series of diblock copolymers and a series of homopolymers to prepare A/B/(C-*block*-D) ternary blends, and then we determined, via cloud point measurement, six interaction parameters needed to interpret experimental results of blend morphology. In this paper we present the highlights of our findings. The organization of this paper is as follows. (i) We will first describe A/B/(C-*block*-D) model ternary blend systems investigated experimentally, including the syntheses of block copolymers and homopolymers. (ii) We will present experimentally determined T_{ODT} of each block copolymer synthesized. (iii) We will present six interaction parameters determined in this study or obtained from the literature for the model ternary blends investigated. (iv) We will present micrographs of ternary blends, obtained from transmission electron microscopy (TEM), for specimens that were melt blended for 5 min at temperatures above and below the T_{ODT} of the block copolymer employed in each ternary blend. (v) We will present TEM images of melt-blended ternary blends that were annealed under isothermal conditions for 12 h at temperatures above and below the T_{ODT} of block copolymer. (vi) We will present micrographs of the rapidly precipitated ternary blends followed by an isothermal annealing for 12 h at temperatures above and below the T_{ODT} of block copolymer. (vii) We will discuss a distinction between emulsifying agent and compatibilizing agent when melt blended with two immiscible homopolymers. (viii) Finally, we will point out the role that the T_{ODT} of block copolymer plays in the compatibilization of two immiscible homopolymers.

Experimental Section

Materials. To prepare model ternary blends, we synthesized, via anionic polymerization, a series of poly(α-methylstyrene)-*block*-polyisoprene (PαMS-*block*-PI) copolymers. The details of the synthesis procedures employed are as follows. Isoprene and α-methyl styrene monomers, separately, were stirred in the presence of calcium hydride (CaH_2) for several days and distilled under vacuum into a flask, and then dibutylmagnesium was added by use of a syringe. All the chemicals were purchased from Aldrich Chemical Co. α-Methylstyrene monomer containing dibutylmagnesium was vacuum distilled again and stored in a volumetric cylinder under vacuum. Tetrahydrofuran (THF) (Fisher Scientific) was stirred in the presence of CaH_2 and distilled under vacuum into a flask, where sodium and benzophenone had been added. Just before polymerization, THF was distilled again into the polymerization reactor which was under vacuum and cooled at −78 °C in a bath of dry ice and 2-propanol, and then the α-methylstyrene monomer was added to the reactor by use of a double-end deflected needle. Polymerization was carried out at −78 °C because of the low ceiling temperature of α-methylstyrene. When a predetermined amount of *sec*-butyllithium (Aldrich Chemical Co.) was added into the reactor by use of a syringe, the color of the solution in the reactor turned red. Polymerization of the α-methylstyrene lasted for 6 h, and then the isoprene monomer containing dibutylmagnesium was distilled under vacuum and directly transferred into the reactor. The color of the solution turned yellow, and the reactor temperature was raised to room temperature. After polymerization of isoprene for 4 h, 1 mL of degassed methanol was injected into the reactor, which caused the solution to become transparent. The solution was precipitated in methanol, and the precipitated PαMS-*block*-PI copolymer was filtered and dried at room temperature in a vacuum oven. Owing to the use of THF as a solvent, PI block of PαMS-*block*-PI copolymer

Table 1. Molecular Characteristics of Diblock Copolymers Synthesized in This Study

sample code	M_n (g/mol)[a]	M_w/M_n[b]	wt % PS or PαMS	T_{ODT} (°C)
MSPI-23[c]	23 000	1.04	51.1	175
MSPI-25[c]	25 000	1.08	50.4	>250
SEB-15[d]	15 000	1.12	52.7	125
SEB-19[e]	19 000	1.04	52.8	258
SB-17[f]	17 000	1.04	53.0	123

[a] Membrane osmometry was employed to determine the number-average molecular weight (M_n). [b] GPC was used to determine polydispersity index, M_w/M_n. [c] PαMS-*block*-PI copolymer having 59% 3,4-addition in PI block. [d] PS-*block*-PEB copolymer having 94% 1-butene in PEB block. [e] PS-*block*-PEB copolymer having 90% 1-butene in PEB block. [f] PS-*block*-PB copolymer having 89% 1,2-addition in PB block.

contained 59% 3,4-addition and 35% 1,2-addition as determined by ^{13}C nuclear magnetic resonance (NMR) spectroscopy. The molecular characteristics of two PαMS-*block*-PI copolymers, MSPI-23 and MSPI-25, are summarized in Table 1. MSPI-23 and MSPI-25 respectively were later used to compatibilize polystyrene (PS) and polybutadiene (PB), forming A/B/(C-*block*-D) model ternary blends.

PαMS-*block*-PI copolymers other than MSPI-23 and MSPI-25 were also synthesized. However, we found that their T_{ODT}'s were either lower than the glass transition temperature (T_g) of PαMS block (ca. 140 °C) as determined by differential scanning calorimetry or much higher than the highest melt blending temperature contemplated (ca. 220 °C) at which thermal degradation and/or cross-linking reactions of PI block might occur, and thus they are not listed in Table 1. It should be mentioned that the T_g of PαMS block of PαMS-*block*-PI copolymer was found to be lower by about 30−45 °C than the T_g of homopolymer PαMS. This is attributable to the plasticizing effect of rubbery PI block in the PαMS-*block*-PI copolymer. Earlier, similar observations were reported on the T_g of PS block of polystyrene-*block*-polyisoprene (SI diblock) copolymer.[30,31] As will be elaborated on below, we have learned that the T_{ODT} of PαMS-*block*-PI copolymer was very sensitive to molecular weight, and there exists a very narrow range of molecular weights that can give rise to T_{ODT} lying between 140 and 220 °C.

Two polystyrene-*block*-polybutadiene (SB diblock) copolymers were supplied to us by Dr. Adel Halasa at Goodyear Tire and Rubber Company. These two SB diblock copolymers were hydrogenated to obtain polystyrene-*block*-poly(ethylene-*co*-1-butene) (SEB diblock) copolymers, SEB-15 and SEB-19, the molecular characteristics of which are summarized in Table 1. The hydrogenation of SB diblock copolymers was carried out by use of the chemical procedure described by Hahn.[32] A brief description of the procedure employed is as follows. A 1000 mL round-bottom three-neck flask was equipped with magnetic stirrer, a reflux condenser, and a stopper. A positive pressure of dry nitrogen was supplied into the reactor through a mineral oil bubbler and the reflux condenser. To the reactor was added ca. 7 g of SB diblock copolymer and 600 mL of *o*-xylene. After the SB diblock copolymer was completely dissolved, 58 g of *p*-toluenesulfonyl hydrazide and 44.5 g of tri-*n*-propylamine were added to the flask. The reactor was heated to reflux at 135−140 °C for 4 h until the color of the reaction solution changed from colorless to deep orange. After hydrogenation was completed, the solution was washed twice with 500 mL of distilled water and filtered through a 0.3 cm layer of activated alumina in a coarse sintered glass filter funnel. The hydrogenated block copolymer was precipitated in methanol. The precipitated block copolymer was dried in a vacuum oven at 90 °C for 12 h. SEB-15 and SEB-19 respectively were later used to compatibilize poly(phenylene oxide) (PPO) and polypropylene (PP), forming A/B/(C-*block*-D) model ternary blends.

A polystyrene-*block*-polybutadiene (SB diblock) copolymer, SB-17, the molecular characteristics of which are summarized in Table 1, was supplied to us by Dr. Adel Halasa at Goodyear Tire and Rubber Company. This block copolymer was later used to compatibilize PαMS and PI, forming A/B/(C-*block*-D) model ternary blends.

Table 2. Molecular Characteristics of Homopolymers Employed in This Study

sample code	M_n (g/mol)	M_w/M_n[j]	M_w (g/mol)
PS-10[a]	1.00×10^4	1.02	1.02×10^4
PI-200[b,c]	1.96×10^5	1.07	2.09×10^5
PB-12[b,d]	1.12×10^4	1.09	1.11×10^4
PB-80[b,d]	7.10×10^4	1.11	7.88×10^4
PαMS-98[e]	8.69×10^4	1.12	9.77×10^4
PPO[f]	0.66×10^4	1.24	0.82×10^4
PMMA[b,g]	0.58×10^5	1.90	1.10×10^5
PS-220[b,h]	1.10×10^5	2.03	2.23×10^5
PP[i]	5.78×10^4	5.88	3.39×10^5

[a] The weight-average molecular weight (M_w) was determined via GPC against PS standards. [b] Membrane osmometry was employed to determine the number-average molecular weight (M_n). [c] It contains 94% 1,4-addition and 6% 3,4-addition. [d] It contains 90% 1,2-addition. [e] Reference 33 reported the value of M_w determined via GPC against the PαMS standards. [f] Experimental grade of poly(phenylene oxide) whose M_w was determined via GPC against the PS standards. [g] Experimental grade of poly(methyl methacrylate). [h] Commercial grade of polystyrene (STYRON 615APR, Dow Chemical Co.) [i] Commercial grade of polypropylene (Escorene 1052, Exxon Chemical Co.) whose M_w was determined by use of high-temperature GPC. [j] GPC was used to determine M_w/M_n.

A homopolystyrene, PS-10, was synthesized, via anionic polymerization, in our laboratory. Dr. Adel Halasa at Goodyear Tire and Rubber Company supplied us with two homopolybutadienes, PB-12 and PB-80, and a homopolyisoprene, PI-200. A poly(α-methylstyrene), PαMS-98, was synthesized earlier by Dr. Jin Kon Kim.[33] A low-molecular-weight poly(phenylene oxide) (PPO) was supplied to us by Dr. Norberto Silvi at General Electric Company. An experimental grade of poly(methyl methacrylate) (PMMA) was supplied to us by Rohm and Haas Company. In addition, two commercial homopolymers were used: (i) polystyrene (STYRON 615APR, Dow Chemical Company) and (ii) polypropylene (PP) (Escorene 1052, Exxon Chemical Company). The molecular characteristics of these homopolymers are summarized in Table 2.

Membrane osmometry (Jupiter Instrument) was used to determine the number-average molecular weight (M_n) of each of the model block copolymers (Table 1) and each of the homopolymers (Table 2), with the exception of PP. High-temperature gel permeation chromatography (GPC) was used to determine the weight-average molecular weight (M_w) of PP, Escorene 1052, against polystyrene standards. The polydispersity (M_w/M_n) of each of the polymers was determined by GPC.

Sample Preparation. Combinations of the diblock copolymers listed in Table 1 and the homopolymers listed in Table 2 were used to prepare the following model ternary blends by melt blending at temperatures above and below the T_{ODT} of each block copolymer: (i) PS/PB/(PαMS-*block*-PI), (ii) PαMS/PI/(PS-*block*-PB), (iii) PPO/PP/(PS-*block*-PEB), and (iv) PMMA/PP/(PαMS-*block*-PI). The blends are summarized in Table 3. In the preparation of ternary blends by melt blending, a Mini-Max mixer was used at a rotor speed of 100 rpm. In all cases, the melt blending temperature of 200 °C and mixing time of 5 min were used. About 1 g of blend sample with a predetermined blend ratio was used to prepare each batch. After melt blending, the blend sample was cooled to room temperature and stored in a freezer.

Also, PS/PB/(PαMS-*block*-PI) and PαMS/PI/(PS-*block*-PB) ternary blends were prepared by rapid precipitation from a homogeneous solution, which were subsequently annealed under isothermal conditions at temperatures above and below the T_{ODT} of block copolymer. For this, two immiscible homopolymers and a block copolymer were dissolved in a common solvent, toluene, and then the homogeneous solution (2 wt % polymer) was stirred for at least 24 h. Then, the solution was

Table 3. A/B/(C-*block*-D) Ternary Blend Systems Investigated in This Study

ternary blend system	interaction parameter
PS/PB/(PαMS-*block*-PI)	$\chi_{PB/PI} < 0$, $\chi_{PS/P\alpha MS} \approx 0$, $\chi_{PS/PB} > 0$, $\chi_{PS/PI} > 0$, $\chi_{PB/P\alpha MS} > 0$, and $\chi_{P\alpha MS/PI} > 0$
PαMS/PI/(PS-*block*-PB)	$\chi_{PB/PI} < 0$, $\chi_{PS/P\alpha MS} \approx 0$, $\chi_{PS/PB} > 0$, $\chi_{PS/PI} > 0$, $\chi_{PB/P\alpha MS} > 0$, and $\chi_{P\alpha MS/PI} > 0$
PPO/PP/(PS-*block*-PEB)	$\chi_{PPO/PS} < 0$, $\chi_{PP/PEB} < 0$, $\chi_{PPO/PP} > 0$, $\chi_{PP/PS} > 0$, $\chi_{PPO/PEB} > 0$, and $\chi_{PS/PEB} > 0$
PMMA/PP/(PαMS-*block*-PI)	$\chi_{PMMA/PP} > 0$, $\chi_{PMMA/P\alpha MS} > 0$, $\chi_{PMMA/PI} > 0$, $\chi_{PP/P\alpha MS} > 0$, $\chi_{PP/PI} > 0$, and $\chi_{P\alpha MS/PI} > 0$

slowly poured into the rapid precipitation setup, which was comprised of a six-blade turbine centrally placed in a perforated draft tube. The rapid precipitation setup was maintained at −78 °C, and the tall form beaker containing both the draft tube and the rotating shaft was charged with methanol. Immediate precipitation of the polymers was observed upon the polymer solution's contact with the circulating methanol pool. The suspension of the precipitated polymers in a liquid blend of toluene and methanol was filtered at room temperature. After filtration, the precipitated polymers were washed several times by methanol to remove toluene. The washed precipitates were dried at room temperature in a fume hood for 1 day and then in a vacuum oven at 40 °C for 1 week to remove residual solvent. All blend samples were then stored in a freezer. The rapidly precipitated blend was annealed in a vacuum oven at a predetermined temperature for varying periods.

Samples for oscillatory shear rheometry for determining the T_{ODT} of block copolymer and TEM study were prepared by first dissolving predetermined amounts of homopolymers and block copolymer (10 wt % in solution) in the presence of 0.1 wt % antioxidant (Irganox 1010, Ciba-Geigy Co.) and then slowly evaporating the solvent. The evaporation of solvent was carried out initially in a fume hood at room temperature for a week and then in a vacuum oven at 40 °C for 3 days. The last trace of solvent was removed by drying the sample in a vacuum oven and gradually raising the oven temperature to 80 °C. Drying of the sample was continued until there was no further change in weight. Finally, the sample was annealed at 110 °C for 10 h.

Cloud Point Measurement. The cloud point of a pair of homopolymers was determined by use of laser light scattering. For this, a glass slide containing a specimen was placed on the hot stage of the sample holder fitted with a programmable temperature controller. A low-power He−Ne laser (wavelength of 635 nm) was used as the light source, and a photodiode was used as the detector. A specimen was first heated to a temperature slightly (ca. 20 °C) above the cloud point (i.e., in the isotropic region) followed by a slow cooling into the two-phase region where a change in light intensity was noticeable. The specimen was then heated again at a preset rate (0.5−5 °C/min), during which information on both temperature and the intensity of scattered light was stored on a computer. For each composition of a particular blend system, cloud point measurements were repeated 3−5 times until data were reproducible, and a fresh specimen was used for each experimental run. For a given blend system, 8−9 compositions from 10/90 to 90/10 blend ratios were used to measure cloud point. The results of cloud point measurement were used to determine the interaction parameter with the aid of the Flory−Huggins theory.

Oscillatory Shear Rheometry. A Rheometrics mechanical spectrometer (model RMS 800) was used in the oscillatory mode with parallel plate fixtures (25 mm diameter) in order to determine the T_{ODT} of block copolymer. Isochronal dynamic temperature sweep experiments were conducted in the heating process, during which the dynamic storage and loss moduli (G' and G'') were measured at an angular frequency (ω) of 0.01 rad/s. The temperature control was accurate to within ±1 °C. All the rheological measurements were conducted under a nitrogen atmosphere in order to preclude oxidative degradation of the samples.

Transmission Electron Microscopy (TEM). The ultrathin sectioning (ca. 50 nm thick) of specimens was performed by cryoultramicrotomy at −100 °C using a Reichert Ultracut S (Leica) microtome equipped with a diamond knife. A transmission electron microscope (JEM 1200 EX II, JEOL) operated at 120 kV was utilized to observe the images of the specimens. Thin sections of specimen were transferred on a copper grid and stained with osmium tetroxide (OsO_4) vapor or ruthenium tetroxide (RuO_4) vapor. OsO_4 was used to stain homopolymer PB-80 and PI block in (PS-220)/(PB-80)/(PαMS-*block*-PI) ternary blend, homopolymer PI-200 and PB block in (PαMS-98)/(PI-200)/(PS-*block*-PB) ternary blend, and PI block in PMMA/PP/(PαMS-*block*-PI) ternary blend. RuO_4 was used to stain homopolymer PPO and PS block in PPO/PP/(PS-*block*-PEB) ternary blend.

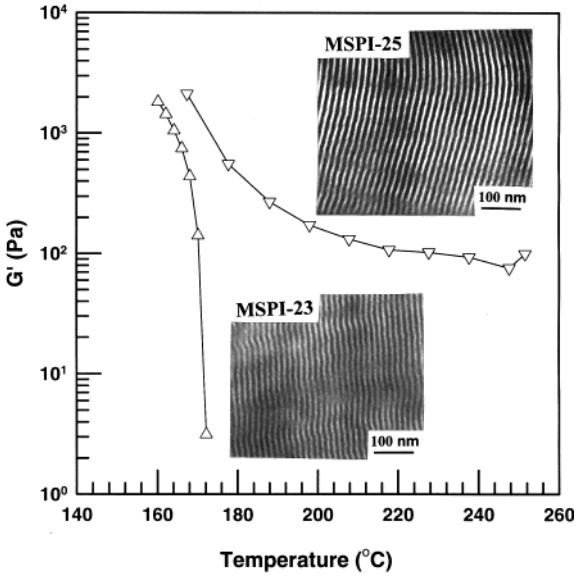

Figure 2. Variation of G' with temperature during the isochronal dynamic temperature sweep experiment at $\omega = 0.01$ rad/s for MSPI-23 (△) and MSPI-25 (▽). Also given are TEM images of MSPI-23 and MSPI-25.

Results

***T_{ODT}*'s and Microdomain Structures of Block Copolymers.** To determine melt blending temperature or annealing temperature of the rapidly precipitated blend specimens, we had to first determine the T_{ODT} of neat block copolymers synthesized. In this study we employed isochronal dynamic temperature sweep experiments to determine T_{ODT}.

Figure 2 describes the temperature dependence of G' for two PαMS-*block*-PI copolymers, MSPI-23 and MSPI-25, which was obtained, during heating, from isochronal dynamic temperature sweep experiments at $\omega = 0.01$ rad/s. According to the literature,[34] T_{ODT} can be determined from a critical temperature at which G' in Figure 2 begins to drop precipitously. Although such a rheological criterion has no theoretical basis, the rationale behind the criterion lies in that microphase-separated block copolymer exhibits solidlike behavior with very high modulus until it reaches, during heating, a certain critical temperature at which the microdomains of block copolymer begin to disappear and exhibits liquidlike behavior. Using such a rheological criterion, from Figure 2 we determine the T_{ODT} of MSPI-23 to be ca. 175 °C and the T_{ODT} of MSPI-25 to be much higher than 250 °C. In Figure 2 we observe that G' for MSPI-25 initially

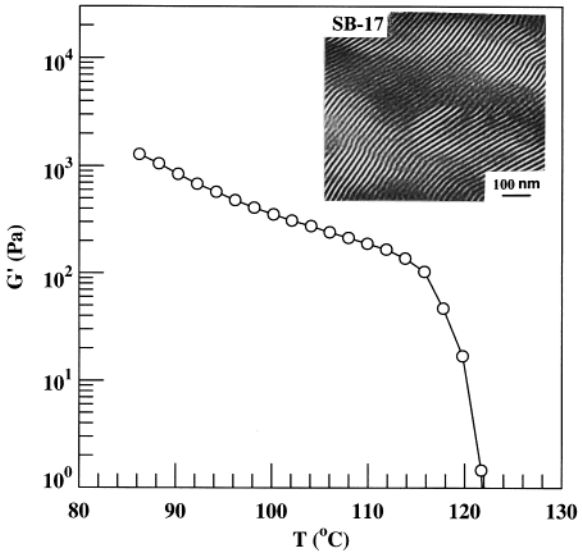

Figure 3. Variation of G' with temperature during the isochronal dynamic temperature sweep experiment at $\omega = 0.01$ rad/s for SB-17 (○). Also given is a TEM image of SB-17.

decreases rapidly with increasing temperature and then at a slower rate until reaching 250 °C, at which G' starts to increase. We believe that a sudden increase of G' at 250 °C for MSPI-25 is due to the occurrence of cross-linking reactions of PI blocks of MSPI-25. Also given in Figure 2 are TEM images of two block copolymers, MSPI-23 and MSPI-25, each having lamellar microdomain structure. This is expected because both block copolymers have almost equal volume fractions (Table 1). It is of great interest to observe in Figure 2 that the T_{ODT} of PαMS-*block*-PI copolymer is extremely sensitive to molecular weight. Specifically, an increase in molecular weight (M_n) from 23 000 (MSPI-23) to 25 000 (MSPI-25) increased T_{ODT} more than 75 °C. The above observations indicate that a very narrow range of molecular weight exists, over which the T_{ODT} of PαMS-*block*-PI copolymer can lie between 140 °C and the thermal degradation/cross-linking temperature (say ca. 220 °C) of PI block. Above we noted that the T_g of PαMS block of PαMS-*block*-PI copolymer is ca. 140 °C.

Figure 3 describes the temperature dependence of G' for a PS-*block*-PB copolymer, SB-17, which was obtained, during heating, from the isochronal dynamic temperature sweep experiment at $\omega = 0.01$ rad/s. From Figure 3 we determine the T_{ODT} of SB-17 to be ca. 122 °C. Note that SB-17 is a nearly symmetric diblock copolymer (Table 1), and thus SB-17 has lamellar microdomain structure as given in Figure 3.

Figure 4 describes the temperature dependence of G' for two PS-*block*-PEB copolymers, SEB-15 and SEB-19, which was obtained, during heating, from the isochronal dynamic temperature sweep experiment at $\omega = 0.01$ rad/s. From Figure 4 we determine $T_{ODT} \approx 125$ °C for SEB-15 and $T_{ODT} \approx 258$ °C for SEB-19. Note that both SEB-15 and SEB-19 are nearly symmetric diblock copolymers (Table 1), and thus they form lamellar microdomain structure as given in Figure 4.

The values of T_{ODT} determined above were the basis on which the melt blending temperature of 200 °C was chosen for the various ternary blends investigated in this study (Table 3). In other words, the choice of 200 °C for melt blending temperature enabled us to prepare ternary blends below and above the T_{ODT} of block copolymers.

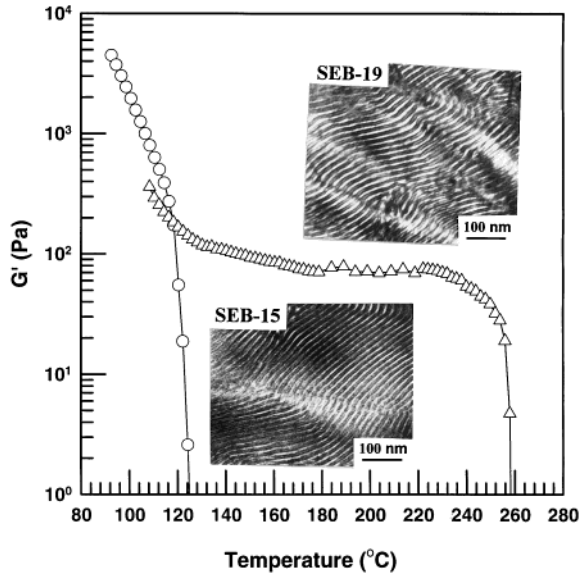

Figure 4. Variation of G' with temperature during the isochronal dynamic temperature sweep experiment at $\omega = 0.01$ rad/s for SEB-15 (○) and SEB-19 (△). Also given are TEM images of SEB-15 and SEB-19.

Table 4. Interaction Parameters Associated with the PS/PB/(PαMS-*block*-PI) and PαMs/PI/(PS-*block*-PB) Ternary Blends

polymer pair	interaction parameter	eq	source
PαMS/PI[a]	$\alpha = -0.1735 \times 10^{-2} + 1.1735/T - 0.0929\phi_{P\alpha MS/PI}/T$	1	this study
PαMS/PS	$\alpha = -0.0028 \times 10^{-2} + 0.0319/T - 0.0009\phi_{P\alpha MS/PS}/T$	2	ref 35
PαMS/PB[b]	$\alpha = -0.5069 \times 10^{-2} + 2.693/T - 0.1368\phi_{P\alpha MS/PB}/T$	3	this study
PS/PI[a]	$\alpha = -0.3188 \times 10^{-2} + 1.6585/T - 0.02018\phi_{PS/PI}/T$	4	this study
PS/PB[b]	$\alpha = -0.1699 \times 10^{-2} + 1.090/T + 0.0351\phi_{PS/PB}/T$	5	ref 36
PI[a]/PB[c]	$\chi = 0.2359 \times 10^{-2} - 5.76/T + 2.22\phi_{PI/PB}/T$	6	this study

[a] For PI containing 59% 3,4-addition. [b] For PB containing 93% 1,2-addition. [c] For PB containing 91% 1,2-addition. $\phi_{P\alpha MS/PI}$, for instance, is the volume fraction of PαMS in the PαMS/PI pair in the PS/PB/(PαMS-*block*-PI) ternary blend: $\phi_{P\alpha MS/PI} = \Phi_{P\alpha MS}/(\Phi_{P\alpha MS} + \Phi_{PI})$ with $\Phi_{P\alpha MS}$ being the volume fraction of PαMS in a given PS/PB/(PαMS-*block*-PI) ternary blend.

Interaction Parameters for the Polymer Pairs Associated with Ternary Blends. To facilitate our discussion later, below we present the interaction parameters determined for the polymer pairs associated with ternary blends investigated in this study. Table 4 gives six expressions for the interaction parameters associated with PS/PB/(PαMS-*block*-PI) and PαMS/PI/(PS-*block*-PB) ternary blends; namely, $\alpha_{P\alpha MS/PI}$, $\alpha_{P\alpha MS/PS}$, $\alpha_{P\alpha MS/PB}$, $\alpha_{PS/PI}$, $\alpha_{PS/PB}$, and $\chi_{PI/PB}$. Note that α is related to χ by $\chi = V_r\alpha$ with V_r being the molar volume of reference component. It should be mentioned that when using experimental results of cloud point measurement, α is obtained with the aid of the Flory−Huggins theory. Equations 1, 3, and 4 in Table 4 were determined in this study from cloud point measurements, while eqs 2 and 5 were taken from the literature.[35,36] Equation 6 in Table 4 was obtained in this study by using regression analysis (see Appendix) of the experimental data reported by Thudium and Han.[37]

Table 5 gives expressions for the interaction parameters associated with PPO/PB/(PS-*block*-PEB) ternary blends; namely, $\chi_{PPO/PS}$, $\chi_{PP/PEB}$, and $\alpha_{PS/PEB}$. Since the

Table 5. Interaction Parameters Associated with the PPO/PP/(PS-*block*-PEB) Ternary Blends

polymer pair	interaction parameter	eq	source
PPO/PS	$\chi_{PPO/PS} = 0.121 - 77.9/T$	7	ref 38
PP/PEB[a]	$\chi_{PP/PEB} = -0.58 \times 10^{-2} + 1.54/T$	8	this study
PS/PEB[b]	$\alpha_{PS/PEB} = -0.6868 \times 10^{-2} + 3.3856/T + 0.0288\phi_{PS}/T$	9	ref 36
PPO/PEB	$\chi > 0$	10	
PS/PP	$\chi > 0$	11	
PPO/PP	$\chi > 0$	12	

[a] PEB containing 90% 1-butene. [b] PEB containing 93% 1-butene.

PEB block of PS-*block*-PEB is a random copolymer consisting of poly(1-butene) (PB-1) and polyethylene (PE), eq 8 in Table 5 was obtained from the following expression:[38,39]

$$\chi_{PP/PEB} = y\chi_{PP/(PB-1)} + (1-y)\chi_{PP/PE} - y(1-y)\chi_{PE/(PB-1)} \quad (13)$$

with $y = 0.9$, where y is the volume fraction of 1-butene in the PEB block of SEB-15 and SEB-19, $\chi_{PP/PB-1}$ is the interaction parameter for the PP/(PB-1) pair, $\chi_{PP/PE}$ is the interaction parameter for the PP/PE pair, and $\chi_{PE/PB-1}$ is the interaction parameter for the PE/(PB-1) pair. We used the following expression

$$\chi_{PP/(PB-1)} = -7.98 \times 10^{-2} + 3.83/T \quad (14)$$

which was obtained in this study by using regression analysis of the experimental data given in Table 4 and eq 5 of ref 40,

$$\chi_{PP/PE} = -2.45 \times 10^{-2} + 16.63/T \quad (15)$$

which is given by eq 9 of ref 41, and

$$\chi_{PE/PB-1} = -5.05 \times 10^{-2} + 39.5/T \quad (16)$$

which was obtained in this study by using regression analysis of the experimental data given in Table 4 of ref 42.

According to eq 9 in Table 5, the 50/50 PS/PEB pair containing 93% 1-butene in PEB, for instance, has $\alpha_{PS/PEB} > 0$ (repulsive interactions) at temperatures until thermal degradation takes place. In view of the fact that, in accordance with eq 7 in Table 5, PPO/PS pairs exhibit lower critical solution temperature and are miscible (i.e., $\chi_{PPO/PS} < 0$) at temperatures below ca. 370 °C, it is then reasonable to speculate that the temperature dependence of $\chi_{PPO/PEB}$ would be very similar to that of $\chi_{PS/PEB}$, i.e., $\chi_{PPO/PEB} > 0$ at any realistic melt blending temperature (say below 350 °C). It has long been established experimentally that PS/PP pair is *not* miscible (i.e., $\chi_{PS/PP} > 0$) at any realistic melt blending temperature before encountering thermal degradation. Thus, it is reasonable to speculate that $\chi_{PPO/PP} > 0$ at any realistic melt blending temperature before encountering thermal degradation. Therefore, we can conclude from the above observations that, for the PPO/PP/(SEB-15) and PPO/PP/(SEB-19) ternary blends investigated in this study, we have $\chi_{PP/PEB} < 0$, $\chi_{PPO/PS} < 0$, $\chi_{PS/PP} > 0$, $\chi_{PPO/PP} > 0$, $\chi_{PS/PEB} > 0$, and $\chi_{PPO/PEB} > 0$.

Morphology of PS/PB/(PαMS-*block*-PI) and PαMS/PI/(PS-*block*-PB) Ternary Blends. Figure 5 gives TEM images of the 63/27/10 (PS-220)/(PB-80)/(MSPI-23) ternary blend, which was prepared by melt blending at 200 °C for 5 min. The numbers 63/27/10 denote weight percents of the components in the blend. It should be remembered that the T_{ODT} of MSPI-23 is 175 °C (Figure 2), and thus the melt blending temperature employed was higher than the T_{ODT} of MSPI-23. The lower panel of Figure 5 is a higher magnification. It is of great interest to observe in the TEM images of Figure 5 that the block copolymer MSPI-23 with a layer thickness of ca. 30 nm covers uniformly the entire surface of the PB droplet dispersed in the PS matrix. It should be mentioned that the lamellar thickness of the block copolymer layer on the surface of the PB droplet in Figure 5 is the same as the lamellar thickness in the neat block copolymers, MSPI-23 and MSPI-25, given in Figure 2. This observation ensures us that the interphase lamellae observed in Figure 5 are real and not artifacts in TEM images.

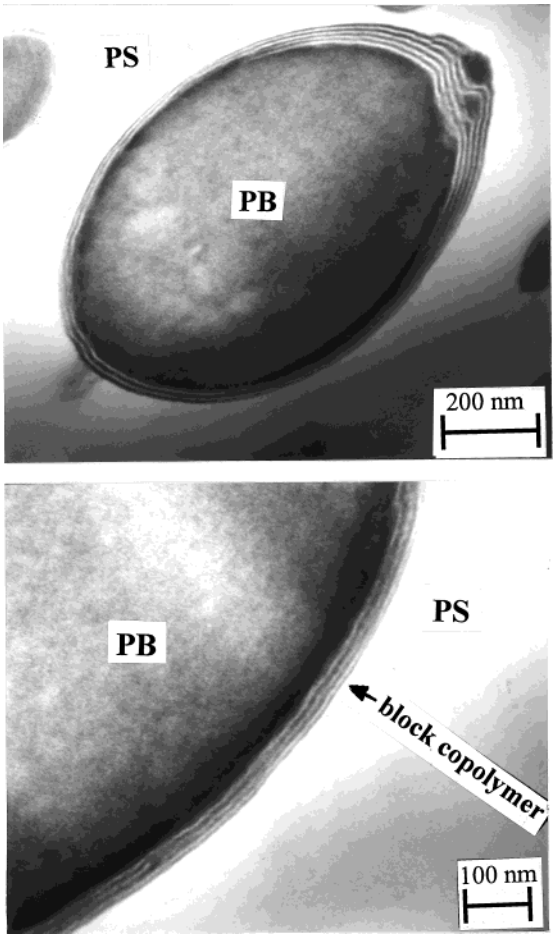

Figure 5. TEM images of the 63/27/10 (PS-220)/(PB-80)/(MSPI-23) ternary blend, which was prepared by melt blending in a Mini-Max mixer for 5 min at 200 °C above the T_{ODT} (175 °C) of MSPI-23. The TEM image in the lower panel is a magnification of that in the upper panel, showing ca. 30 nm thick layer of the block copolymer MSPI-23 located at the (PS-220)/(PB-80) interface.

Figure 6 gives a TEM image of the 63/27/10 (PS-220)/(PB-80)/(MSPI-23) ternary blend, which was annealed at 200 °C for 12 h after being melt blended at 200 °C for 5 min. Again, the annealing temperature employed is higher than the T_{ODT} of MSPI-23. Interestingly, in Figure 6 we observe that the block copolymer MSPI-23, which had uniformly been distributed on the surface of the PB droplet during melt blending, diffused into the PB droplet during isothermal annealing for 12 h at 200 °C, giving rise to an equilibrium morphology representing a homogeneously mixed (PB-80)/(MSPI-23)

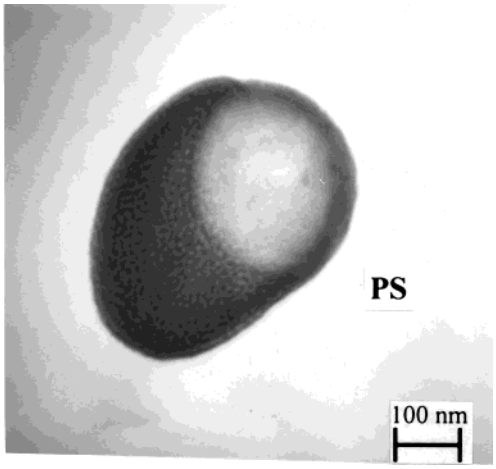

Figure 6. TEM image of the melt-blended 63/27/10 (PS-220)/(PB-80)/(MSPI-23) ternary blend after annealing for 12 h at 200 °C above the T_{ODT} (175 °C) of MSPI-23. The dark areas represent a PB-80 droplet in which PB-80 and MSPI-23 are mixed at a segmental level.

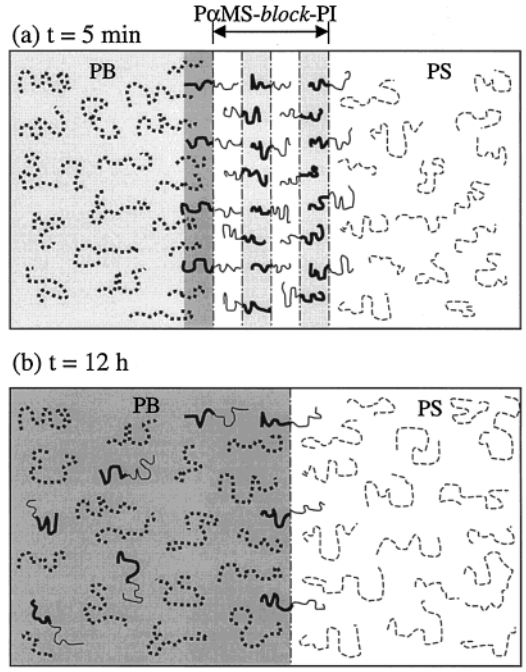

Figure 7. Schematic diagram describing the distributions of components in the 63/27/10 (PS-220)/(PB-80)/(MSPI-23) ternary blend (a) after melt blending at 200 °C for 5 min and (b) after isothermal annealing at 200 °C for 12 h of melt-blended specimen: (—) PI block chain; (−) PαMS block chain; (···) homopolymer PB chain; (- - -) homopolymer PS chain.

blend. This is attributable to the attractive interactions (i.e., $\chi_{PI/PB} < 0$) existing between homopolymer PB-80 and PI block of MSPI-23.

To explain the morphologies, given in Figures 5 and 6, of the 63/27/10 (PS-220)/(PB-80)/(MSPI-23) ternary blend, we prepared a schematic diagram given in Figure 7. Figure 7a describes schematically the distribution of component polymers after melt blending at 200 °C for 5 min, where the light shaded areas represent the chains of homopolymer PB-80 and the chains of PI block of PαMS-*block*-PI copolymer (MSPI-23), each stained by OsO_4, and the dark areas represent a newly formed interphase consisting of the chains of homopolymer PB-80 and the chains of PI block of MSPI-23. The block copolymer chains in the middle of Figure 7a depict a

Table 6. Values of χ at 200 °C for Polymer Pairs Associated with the 63/27/10 (PS-220)/(PB-80)/(MSPI-23) Ternary Blend

polymer pair	χ at 200 °C	source	polymer pair	χ at 200 °C	source
PαMS/PI	0.080	eq 1	PS/PI	0.030	eq 4
PS/PαMS	0.004	eq 2	PS/PB	0.070	eq 5
PαMS/PB	0.068	eq 3	PB/PI	−0.006	eq 6

thin layer of MSPI-23. We speculate that during melt blending at 200 °C ($> T_{ODT}$ of MSPI-23) the homogeneous molecules of MSPI-23 covered the entire surface of PB-80 droplets and formed a block copolymer film with a thickness of ca. 30 nm at the PS/PB interface. This was possible because attractive interactions ($\chi_{PI/PB} < 0$) existed between homopolymer PB-80 and PI block of MSPI-23. When the ternary blend was cooled to room temperature after melt blending, microphase separation of MSPI-23 occurred at the (PS-220)/(PB-80) interface, giving rise to alternating layers of lamellar microdomain structure, shown in the TEM image of Figure 5. Presumably, an interphase consisting of the chains of homopolymer PS-220 and the chains of PαMS block of MSPI-23 might have been formed during melt blending. Such an interphase cannot be discerned in the TEM image of Figure 5, because homopolymer PS-220 and the PαMS block of MSPI-23 were not stained by OsO_4.

Figure 7b describes schematically the distribution of component polymers after the melt-blended 63/27/10 (PS-220)/(PB-80)/(MSPI-23) specimen was annealed at 200 °C for 12 h, where the dark areas on the left side represent a homogeneous mixture consisting of homopolymer PB-80 and MSPI-23, which was formed during isothermal annealing at 200 °C for 12 h. Note that the chains of homopolymer PB-80 and the chains of PI block of MSPI-23 were stained by OsO_4. We speculate that during isothermal annealing all of the MSPI-23 molecules, which had been distributed uniformly on the surface of PB-80 droplets during melt blending, diffused into the PB-80 droplet forming an equilibrium morphology, owing to the attractive interactions existing between homopolymer PB-80 and PI block of MSPI-23. Table 6 summarizes values of χ at 200 °C for polymer pairs associated with the 63/27/10 (PS-220)/(PB-80)/(MSPI-23) ternary blend. Note that the values of χ in Table 6 were obtained from the expressions for the interaction parameters given in Table 4. In Table 6 we observe $\chi_{PB/PI} = -0.006$ and $\chi_{PS/P\alpha MS} = 0.004$. We speculate further that owing to the repulsive interactions, though very weak, between homopolymer PS-200 and PαMS block of MSPI-23 ($\chi_{PS/P\alpha MS} > 0$), all of the molecules of MSPI-23 were dragged into PB-80 droplets during the isothermal annealing, suggesting that the attractive interactions between homopolymer PB-80 and PI block of MSPI-23 played the predominant role in the formation of the equilibrium morphology depicted in Figure 7b.

Figure 8a gives a TEM image of the 63/27/10 (PS-220)/(PB-80)/(MSPI-25) ternary blend, which was prepared by melt blending at 200 °C for 5 min. Note that the melt blending temperature (200 °C) employed is lower than the T_{ODT} (250 °C) of MSPI-25. The TEM image given in Figure 8a shows that MSPI-25 and PB-800 formed separate domains and dispersed in the PS matrix. It is clear that MSPI-25 is *not* uniformly distributed on the surface of the PB droplet. Figure 8b gives a TEM image of the 63/27/10 (PS-220)/(PB-80)/

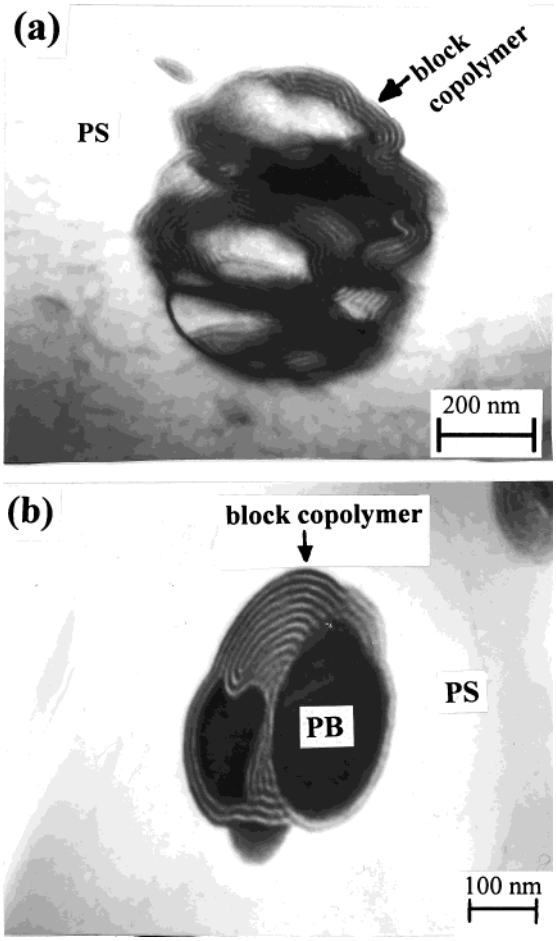

Figure 8. (a) TEM image of the 63/27/10 (PS-220)/(PB-80)/(MSPI-25) ternary blend, which was prepared by melt blending in a Mini-Max mixer for 5 min at 200 °C below the T_{ODT} (>250 °C) of MSPI-25. The dark areas represent the block copolymer MSPI-25. (b) TEM image of the melt-blended 63/27/10 (PS-220)/(PB-80)/(MSPI-25) ternary blend after annealing for 12 h at 200 °C below the T_{ODT} (>250 °C) of MSPI-25.

(MSPI-25) ternary blend, which was annealed at 200 °C for 12 h after being melt blended at 200 °C for 5 min. Note that the annealing temperature employed is lower than the T_{ODT} of MSPI-25. It can be seen in the TEM image of Figure 8b that there is no evidence that MSPI-25 diffused into the PB droplet.

From the observations made above on the TEM images of Figures 5, 6, and 8 we can tentatively conclude that the T_{ODT} of PαMS-*block*-PI copolymer, in relation to melt blending temperature, played the decisive role in determining whether the block copolymer can be distributed uniformly at the PS/PB interface. This can be explained by the differences in viscosity between MSPI-23 and MSPI-25 at 200 °C. Figure 9 gives the temperature dependence of complex viscosity $|\eta^*|$ curves for MSPI-23 and MSPI-25, which were obtained from the isochronal dynamic temperature sweep experiments at $\omega = 0.01$ rad/s. Note that $|\eta^*|$ was calculated from $|\eta^*| = [(G'/w)^2 + (G''/w)^2]^{1/2}$. It can be seen in Figure 9 that at 200 °C the viscosity of MSPI-23 is exceedingly low and the viscosity of MSPI-25 is very high (2×10^4 Pa s). It should be remembered that the molecular weight of MSPI-25 is only ca. 2000 g/mol higher than that of MSPI-23 (Table 1), and therefore such a large difference in viscosity between MSPI-23 and MSPI-25 cannot possibly be due to the difference in molecular weight. Rather, it is due to the difference in the

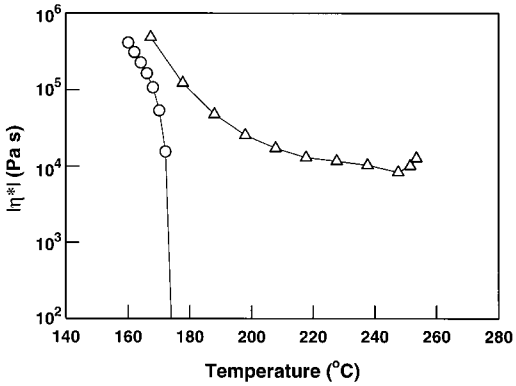

Figure 9. Temperature dependence of complex viscosity $|\eta^*|$ for MSPI-23 (○) and MSPI-25 (△) at an angular frequency ω of 0.01 rad/s.

morphological state of the two block copolymers at 200 °C (MSPI-23 in the disordered state and MSPI-25 in the microphase-separated state). Thus, we conclude that the difference in viscosity between MSPI-23 and MSPI-25 is attributable to the observed difference in the distributions (or locations) of the block copolymer (compare Figure 5 with Figure 8) when melt blended with two immiscible homopolymers, PS-220 and PB-80. That is, at 200 °C the viscosity of MSPI-25 was so high that it had very limited mobility during melt blending, while the viscosity of MSPI-23 was so low that it could easily flow during melt blending and thus spread over the entire surface of PB-80 droplets. The above observations have a profound implication, conceptually and practically, in that the attractive thermodynamic interactions alone are not sufficient, though necessary, for a block copolymer to function as an effective compatibilizing agent for two immiscible homopolymers.

Figure 10a gives a TEM image of the rapidly precipitated 35/15/50 (PS-10)/(PB-12)/(MSPI-23) ternary blend which was annealed for 12 h at 200 °C (above the T_{ODT} of MSPI-23), and Figure 10b gives a TEM image of the same blend which was annealed for 12 h at 160 °C (below the T_{ODT} of MSPI-23). The TEM images in parts a and b of Figure 10 show that the annealing temperature employed, in relation to the T_{ODT} of MSPI-23, played the decisive role in determining the distributions of MSPI-23 in (PS-10)/(PB-12)/(MSPI-23) ternary blend. Specifically, Figure 10a shows that when the rapidly precipitated 35/15/50 (PS-10)/(PB-12)/(MSPI-23) ternary blend was annealed at 200 °C for 12 h, MSPI-23 diffused into the discrete phase of PB-12, giving rise to an equilibrium morphology (the dark areas) which looks very similar to that given in Figure 6. On the other hand, as shown in Figure 10b, no mixing on a segmental level occurred when the same ternary blend was annealed for 12 h at 160 °C which is below the T_{ODT} of MSPI-23. It is clearly seen in Figure 10b that lamellar microdomains of MSPI-23 persisted after the isothermal annealing at 160 °C for 12 h. The readers are reminded that the molecular weights of PS-10 and PB-12 are quite low compared to the molecular weights of PS-220 and PB-80 (Table 2). Therefore, we can conclude that the poor distribution of MSPI-25 observed in the 63/27/10 (PS-220)/(PB-80)/(MSPI-25) ternary blend has little to do with the molecular weights of PS-200 and PB-80 (Figure 8).

We also took TEM images of the rapidly precipitated 63/27/10 (PS-10)/(PB-12)/(MSPI-23) ternary blend after being annealed for 12 h at 200 °C (above the T_{ODT} of

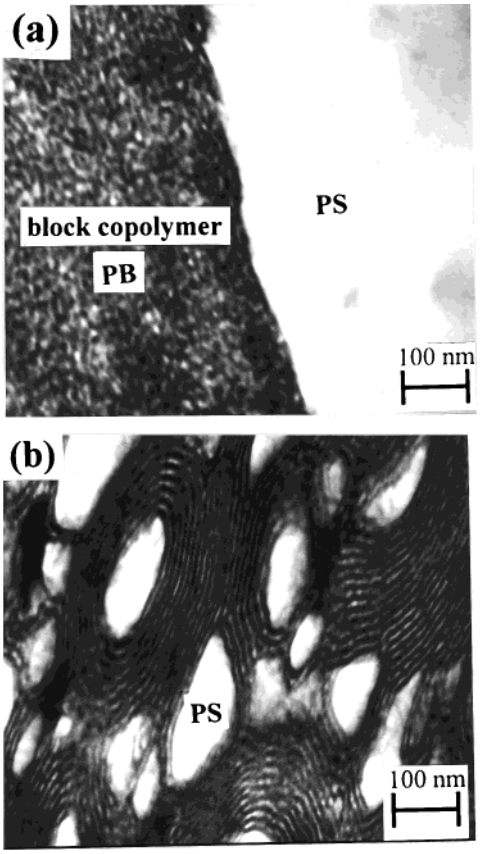

Figure 10. (a) TEM images of the rapidly precipitated 35/15/50 (PS-10)/(PB-12)/(MSPI-23) ternary blend after annealing for 12 h at 200 °C above the T_{ODT} (175 °C) of MSPI-23 and (b) at 160 °C below the T_{ODT} (175 °C) of MSPI-23.

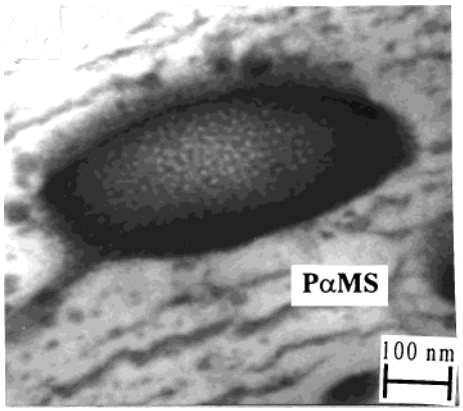

Figure 11. TEM image of the rapidly precipitated 63/27/10 (PαMS-98)/(PI-200)/(SB-17) ternary blend after annealing for 12 h at 190 °C above the T_{ODT} (123 °C) of SB-17. The dark areas represent a PI-200 droplet in which PI-200 and SB-17 are mixed at a segmental level.

MSPI-23). We observed, not presented here, that during isothermal annealing MSPI-23 diffused into PB-12 droplet, giving rise to an equilibrium morphology, very similar to the morphology given in Figure 6.

Figure 11 gives a TEM image of the rapidly precipitated 63/27/10 (PαMS-98)/(PI-200)/(SB-17) ternary blend, which was annealed for 12 h at 190 °C (above the T_{ODT} of SB-17). This ternary blend is a reverse situation of the 63/27/10 (PS-220)/(PB-80)/(MSPI-27) ternary blend with regard to the chemical structures of two homopolymers and block copolymer. We observe that the morphology of the 63/27/10 (PαMS-98)/(PI-200)/(SB-17)

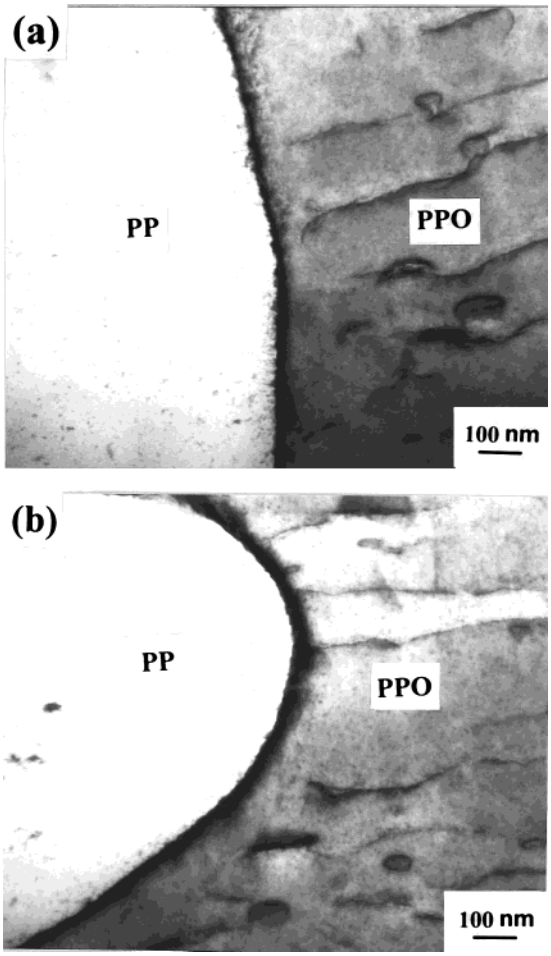

Figure 12. (a) TEM image of the 63/27/10 PPO/PP/(SEB-15) ternary blend which was prepared by melt blending in a Mini-Max mixer for 5 min at 200 °C above the T_{ODT} (125 °C) of SEB-15. (b) TEM image of the melt-blended 63/27/10 PPO/PP/(SEB-15) ternary blend after annealing for 12 h at 200 °C above the T_{ODT} (125 °C) of SEB-15. In both TEM images the block copolymer SEB-15 (the dark layer) is located at the PPO/PO interface.

ternary blend looks very similar to that of the 63/27/10 (PS-220)/(PB-80)/(MSPI-23) (Figure 6).

Morphology of PPO/PP/(PS-*block*-PEB) Ternary Blends. Figure 12a gives a TEM image of the 63/27/10 PPO/PP/(SEB-15) ternary blend which was prepared by melt blending for 5 min at 200 °C, which is higher than the T_{ODT} (125 °C) of SEB-15 (Figure 4). In Figure 12a the bright areas represent the PP phase, the gray areas in the matrix represent the PPO phase, and the dark areas inside the PPO matrix represent SEB-15 droplets. Note that the major component (PPO) forms the continuous phase and that the minor component (PP) forms the discrete phase (i.e., droplets) during melt blending. Note in Figure 12a that an interphase was formed and distributed uniformly at the PPO/PP interface. Figure 12b gives a TEM image of the melt-blended 63/27/10 PPO/PP/(SEB-15) which was subsequently annealed for 12 h at 200 °C, which is higher than the T_{ODT} of SEB-15. In Figure 12b we observe evidence showing that the interphase broadened during the isothermal annealing.

To explain the morphologies, given in Figure 12, of the 63/27/10 PPO/PP/(SEB-15) ternary blend, we prepared a schematic diagram given in Figure 13. Figure 13a describes schematically the distribution of component polymers after melt blending at 200 °C for 5 min,

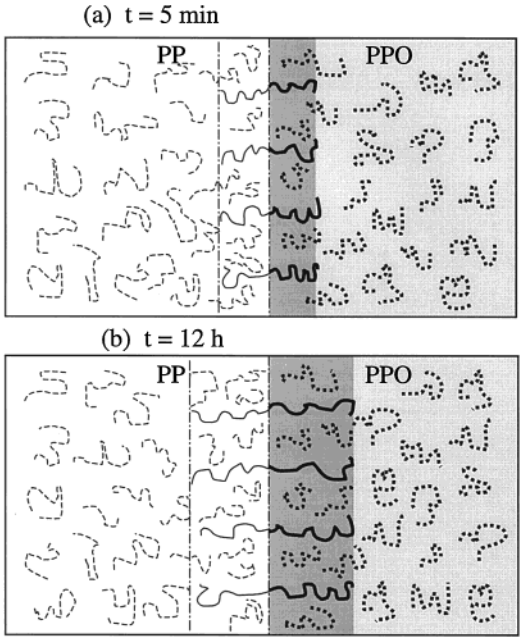

Figure 13. Schematic diagram describing the distributions of components in the 63/27/10 PPO/PP/ (SEB-15) ternary blend (a) after melt blending at 200 °C for 5 min and (b) after isothermal annealing at 200 °C for 12 of melt-blended specimen: (—) PS block chain; (−) PEB block chain; (···) homopolymer PPO chain; (- - -) homopolymer PP chain.

Table 7. Values of χ at 200 °C for Polymer Pairs Associated with the 63/27/10 PPO/PP/(SEB-15) Ternary Blend

polymer pair	χ at 200 °C	source	polymer pair	χ at 200 °C	source
PPO/PS	−0.043	eq 7	PPO/PEB	>0	eq 10
PP/PEB	−0.002	eq 8	PS/PP	>0	eq 11
PS/PEB	0.030	eq 9	PPO/PP	>0	eq 12

where the light shaded areas represent the chains of homopolymer PPO stained by RuO_4 and the dark areas represent a newly formed interphase that consists of homopolymer PPO and PS block of SEB-15. Note that both PPO and PS phases were stained by RuO_4. We are certain that an interphase consisting of the chains of homopolymer PP and the chains of PEB block of SEB-15 must have been formed during melt blending at 200 °C for 5 min, because they have attractive interactions (i.e., $\chi_{PP/PEB} < 0$). But such an interphase cannot be discerned in the TEM image of Figure 12, because homopolymer PP and PEB block of SEB-19 were not stained by RuO_4. Therefore, on the left side of the dark areas in Figure 13a, a vertical broken line is drawn to indicate an interphase consisting of the chains of homopolymer PP and the chains of PEB block of SEB-15. Table 7 summarizes values of χ at 200 °C for the polymer pairs associated with the 63/27/10 PPO/PP/(SEB-15) ternary blend. Note that values of χ at 200 °C given in Table 7 were obtained from the expressions for the interaction parameters given in Table 5. It should be remembered that PEB block of SEB-15 is a random copolymer consisting of ethylene and 1-butene and that the miscibility between homopolymer PP and PEB block of SEB-15 depends on the microstructure of PEB. In Table 7 we observe $\chi_{PP/PEB} = -0.002$ at the melt blending temperature of 200 °C, leading us to conclude that PP/PEB pairs are miscible on a segmental level. Since the melt blending temperature (200 °C) employed was much higher than the T_{ODT} (125 °C) of SEB-15, it is reasonable to speculate that, during melt blending, the chains of PEB block of SEB-15 were stretched preferentially to the surface of the PP phase that formed droplets. In Table 7 we observe $\chi_{PPO/PS} = -0.043$ at 200 °C. Thus, it is reasonable to speculate that during melt blending at 200 °C the chains of PS block of SEB-15 must have been mixed with the chains of homopolymer PPO on a segmental level, forming an interphase. The above observations now seem to explain the morphology of the 63/27/10 PPO/PP/(SEB-15) ternary blend given in Figure 12, i.e., the formation of an interphase (the dark areas) at the PPO/PP interface.

Figure 13b describes schematically the distribution of component polymers after the melt-blended 63/27/10 PPO/PP/(SEB-15) was annealed at 200 °C for 12 h. We speculate that during isothermal annealing at 200 °C, which is higher than the T_{ODT} of SEB-15, the flexible chains of PS block continued to stretch toward the PPO phase and that the flexible chains of PEB block continued to stretch toward the PP phase. The reason is that attractive interactions existed between PPO and PS chains ($\alpha_{PPO/PS} < 0$) and between PP and PEB chains ($\alpha_{PP/PEB} < 0$). Hence, the thickness of the interphase on both sides was broadened during the isothermal annealing as indicated in Figure 13b. Since the chains of each block of SEB-15 were stretched in opposite directions, the overall SEB-15 chains could not be dragged preferentially to a particular homopolymer. Thus, the position of the newly formed interphase stayed more or less in the middle of the PPO and PP phases.

Figure 14a gives a TEM image of the 63/27/10 PPO/PP/(SEB-19) ternary blend which was prepared by melt blending for 5 min at 200 °C, which is lower than the T_{ODT} (258 °C) of SEB-19. The TEM image in Figure 14a shows a very sharp interface between the PP and PPO phases with little evidence of the formation of an interphase. Notice in Figure 14a that the block copolymer SEB-19 (the dark areas) formed separate domains dispersed in the PPO phase (the gray areas). Figure 14b gives a TEM image of the 63/27/10 PPO/PP/(SEB-19) ternary blend which was annealed for 12 h at 200 °C after being melt blended for 5 min at 200 °C (below the T_{ODT} of SEB-19). In Figure 14b we observe little change in blend morphology after a prolonged isothermal annealing at 200 °C.

We can now explain the differences in blend morphology observed in Figures 12 and 14 by the differences in viscosity between SEB-15 and SEB-19 at 200 °C. Figure 15 describes the temperature dependence of $|\eta^*|$ for SEB-15 and SEB-19. It can be seen in Figure 15 that at 200 °C the viscosity of SEB-15 is exceedingly low and the viscosity of SEB-19 is very high (8×10^3 Pa s). It should be remembered that the molecular weight of SEB-19 is only ca. 4000 g/mol higher than that of SEB-15 (Table 1), and therefore such a large difference in viscosity between SEB-15 and SEB-19 cannot possibly be due to the difference in molecular weight. Rather, it is due to the difference in the morphological state of the two block copolymers: SEB-15 in the disordered state and SEB-19 in the microphase-separated state. Thus, we conclude that the difference in viscosity between SEB-15 and SEB-19 is attributable to the observed difference in the distributions (or locations) of block copolymer in the respective ternary blends (compare Figure 12 with Figure 14).

It should be pointed out at this juncture that the microstructure of PEB block of PS-*block*-PEB copolymer

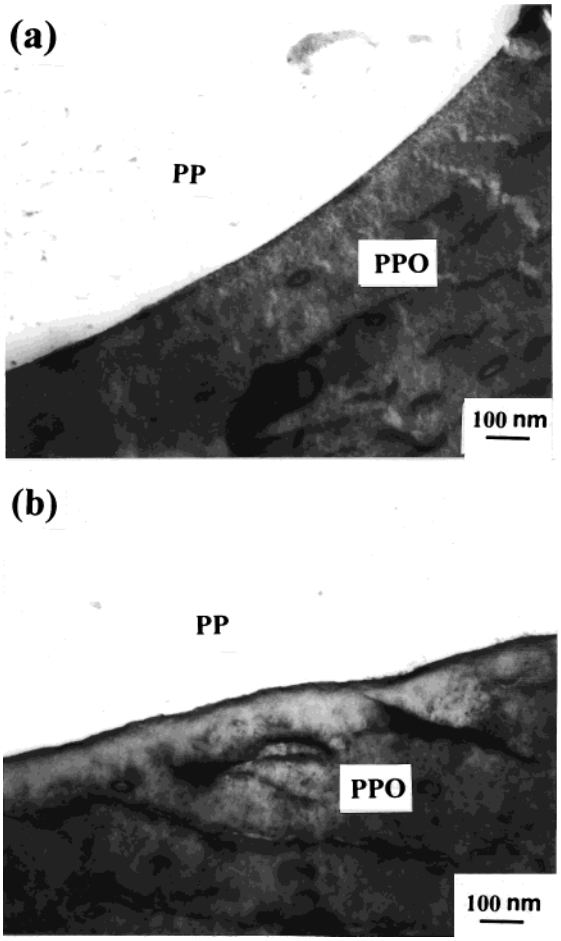

Figure 14. (a) TEM image of the 63/27/10 PPO/PP/(SEB-19) ternary blend which was prepared by melt blending in a Mini-Max mixer for 5 min at 200 °C below the T_{ODT} (258 °C) of SEB-19. There is no evidence of the presence of the block copolymer SEB-19 at the PPO/PP interface, and SEB-19 forms the discrete phase (the very dark areas) and is dispersed in the PPO matrix (the gray areas). (b) TEM image of the melt-blended 63/27/10 PPO/PP/(SEB-19) ternary blend after annealing for 12 h at 200 °C below the T_{ODT} (258 °C) of SEB-19. The block copolymer SEB-19 appears to have migrated to the PPO/PP interface after annealing for 12 h while most of the SEB-19 forming the discrete phase (the dark areas) still reside in the PPO matrix (the gray areas).

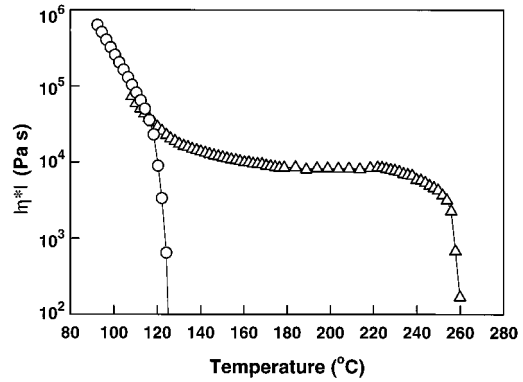

Figure 15. Temperature dependence of complex viscosity $|\eta^*|$ for SEB-15 (○) and SEB-19 (△) at an angular frequency ω of 0.01 rad/s.

plays a very important role in determining the morphology of PPO/PP/(PS-*block*-PEB) ternary blends and thus in the compatibilization of PPO/PP binary blends. This is because the extent of miscibility between homopolymer PP and PEB block of PS-*block*-PEB depends on the microstructure of the PEB block. It should be remembered that the PEB blocks of SEB-15 and SEB-19 have very high 1-butene contents (Table 1) and that PEB with low 1-butene content is very close to polyethylene (PE).

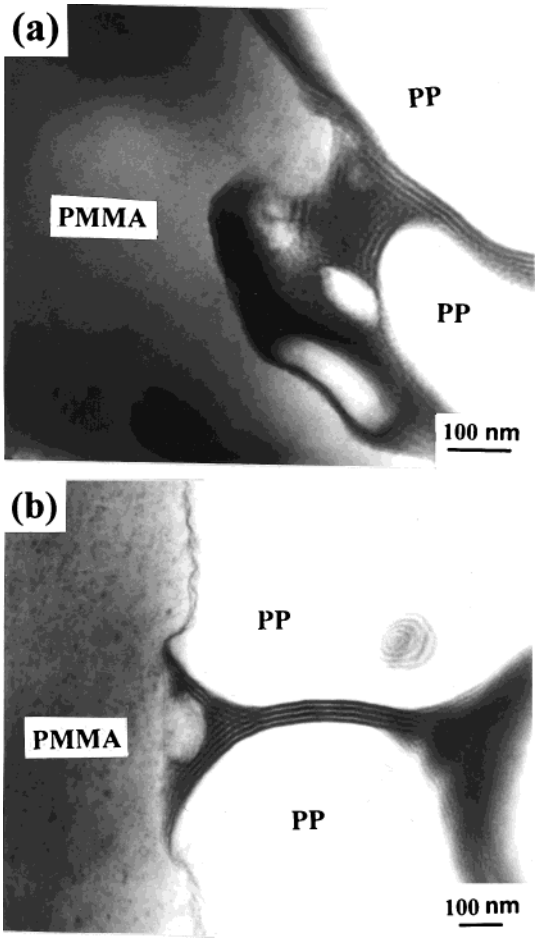

Figure 16. (a) TEM image of the 63/27/10 PMMA/PP/(MSPI-23) ternary blend, which was prepared by melt blending for 5 min at 200 °C above the T_{ODT} (175 °C) of MSPI-23. The block copolymer MSPI-23 forms separate domains dispersed in the PMMA matrix. (b) TEM image of the melt-blended 63/27/10 PMMA/PP/(MSPI-23) ternary blend after annealing for 12 h at 200 °C above the T_{ODT} (175 °C) of MSPI-23. There is no evidence of the presence of the block copolymer MSPI-23 at the PMMA/PP interface.

Morphology of PMMA/PP/(PαMS-*block*-PI) Ternary Blends. For comparison, we also investigated the morphology of the 63/27/10 PMMA/PP/(MSPI-23) ternary blend. Figure 16a gives a TEM image of the blend, which was prepared by melt blending at 200 °C for 5 min. It should be remembered that the T_{ODT} of MSPI-23 is ca. 175 °C (Figure 2), and thus the melt blending temperature employed is higher than the T_{ODT} of MSPI-23. The TEM image of Figure 16a shows that MSPI−23 is *not* located at the PMMA/PP interface, but rather formed separate domains. Figure 16b gives a TEM image of the 63/27/10 PMMA/PP/(MSPI-23) ternary blend, which was annealed at 200 °C for 12 h after being melt blended at 200 °C for 5 min. In Figure 16b we observe hardly any distribution of MSPI-23 at the PMMA/PP interface even after being annealed for 12 h for 200 °C, which is higher than the T_{ODT} of MSPI-23. The above observations should not surprise us, because all six interaction parameters associated with this ternary blend are positive: $\chi_{PMMA/P\alpha MA} > 0$, $\chi_{PMMA/PP} > 0$, $\chi_{PMMA/PI} > 0$, $\chi_{PP/P\alpha MS} > 0$, $\chi_{PP/PI} > 0$, and $\chi_{P\alpha MS/PI} > 0$.

Table 8. Molecular Parameters of the PS-*block*-PMMA Copolymers Employed by Various Investigators for Preparing Ternary Blends with Two Immiscible Homopolymers or Random Copolymers

sample code	M_w (g/mol)	PS (wt frac)	ref
P(S-*b*-MMA)-1	8.7×10^4	NA[a]	1
P(S-*b*-MMA)-2	3.3×10^4	NA[a]	1
BM	9.6×10^4	0.64	7
SM	9.2×10^4	0.57	8
SM78	19.4×10^4	0.47	10
SM8	1.7×10^4	0.44	11
SM25	6.1×10^4	0.47	11
SM43	8.2×10^4	0.48	11
SM78	14.8×10^4	0.47	11
SM97	20.3×10^4	0.47	11
SM120	25.8×10^4	0.40	11
PS-*b*-PMMA	33.4×10^4	0.48	12
SM-3	29.4×10^4 [b]	0.50	43
SM55	5.8×10^4	0.58	44
SM85	8.9×10^4	0.55	44
SM160	10.8×10^4	0.50	44
SM780	96.7×10^4	0.40	44
B65	6.6×10^4	0.50	45
B283	28.3×10^4	0.43	45
B680	68.0×10^4	0.67	45
B1170	117.0×10^4	0.75	45

[a] Not available. [b] Since ref 43 provided with the value of M_n only, the value of M_w given here is estimated by assuming $M_w/M_n = 1.05$.

Discussion

In the past, numerous research groups[1,5−8,10−12,43−45] have used PS-*block*-PMMA copolymers to investigate the emulsification and/or compatibilization of two immiscible homopolymers PS and PMMA (belonging to A/B/(A-*block*-B) ternary blend) or two immiscible homopolymers C and D whose chemical structures are different from those of PS and PMMA blocks (belonging to A/B/(C-*block*-D) ternary blend). Some investigators[3,12,43−45] concluded that their PS-*block*-PMMA copolymers played the role of emulsifying agents on the basis of the reduction in size of the discrete phase of PS/PMMA or C/D binary blends, while others[7,8,10,11] concluded that their PS-*block*-PMMA copolymers played the role of compatibilizing agent on the basis of some improvement in certain mechanical properties. Table 8 gives a summary of the molecular weights of the PS-*block*-PMMA copolymers employed for such purposes by various research groups.

Using information on the molecular weight given in Table 8, we estimated the T_{ODT}'s of the PS-*block*-PMMA copolymers with the aid of the Leibler theory,[46] for which the following expression,

$$\chi_{PS/PMMA} = (0.028 \pm 0.002) + (3.9 \pm 0.6)/T \quad (17)$$

was used, which was reported by Russell et al.,[47] who measured the small-angle neutron scattering from compositionally symmetric PS-*block*-PMMA copolymers at temperatures above T_{ODT}. In obtaining eq 17, Russell et al. varied χ to produce the best fit, with the aid of the Leibler theory,[46] to the experimental scattering profiles at different temperatures. We found that the estimated values of T_{ODT} were very sensitive to the molecular weight of PS-*block*-PMMA copolymer, as summarized in Table 9. From Table 9 we conclude that almost all of the PS-*block*-PMMA copolymers, with the exception of SM8, would have had T_{ODT} far exceeding the melt blending temperatures employed (say 300 °C as the highest value). This observation suggests that the PS-*block*-PMMA copolymers employed by various research groups could not have formed an interphase during melt blending and thus could not have played the role of compatibilizing agent. However, such block copolymers might have played the role of emulsifying agent to reduce the domain size. Some investigators[43−45] reported that PS-*block*-PMMA copolymers helped to slow the rate of droplet coalescence or prevent coalescence of droplets in their ternary blends.

Table 9. T_{ODT} of Compositionally Symmetric PS-*block*-PMMA Copolymers Predicted from the Leibler Theory

M_w (g/mol)	T_{ODT} (°C)[a]	M_w (g/mol)	T_{ODT} (°C)[a]
2.0×10^4	−122	3.2×10^4	416
2.4×10^4	−42	3.4×10^4	774
2.8×10^4	100	3.6×10^4	1544

[a] Equation 17 was used to predict T_{ODT}.

Table 10. Molecular Parameters of the SEB and SEBS Block Copolymers Employed by Various Investigators for Preparing Ternary Blends with Two Immiscible Homopolymers

sample code	M_w (g/mol)	PS (wt frac)	ref	predicted T_{ODT} (°C)[a]
(a) SEB				
SE-2[b]	16.3×10^4 [c]	0.49	3c	426
SE-5[b]	8.4×10^4 [c]	0.50	3c	397
SE-1[b]	6.1×10^4 [c]	0.43	3f	373
SE-3[b]	28.9×10^4 [c]	0.50	3f	439
(b) SEBS				
Kraton G1652	8.7×10^4 [d]	0.29	4a, 4c, 4d, 4f, 4g, 4h	316

[a] Equation 20 was used to predict T_{ODT} from the Helfand−Wasserman theory. [b] The amount of 1-butene in the PEB block was not provided in refs 3c and 3f. [c] Since refs 3c and 3f provided with values of M_n only, values of M_w given here are estimated by assuming $M_w/M_n = 1.05$. [d] Taken from ref 4h.

Some investigators[3] used SEB diblock copolymers, and others[4] used polystyrene-*block*-poly(ethylene-*co*-1-butene)-*block*-polystyrene (SEBS triblock) copolymers, to emulsify or compatibilize such immiscible binary blends, as PS/low-density polyethylene (LDPE), high-density polyethylene (HDPE)/poly(ethylene terephthalate) (PET), polypropylene (PP)/HDPE, PS/PP, or PPO/PP. Table 10 gives a summary of the molecular weights of the SEB and SEBS block copolymers employed for such purposes by various research groups.[3,4]

Using information on the molecular weight given in Table 10, we estimated the T_{ODT}'s of SEB and SEBS block copolymers with the aid of the Helfand−Wasserman theory,[48] for which the following expression[36] was used:

$$\alpha_{PS/PEB} = -0.1678 \times 10^{-2} + 1.2536/T - 0.0648\phi_{PS}/T \quad (18)$$

where α is related to χ by $\chi = \alpha V_r$ with V_r being the molar volume of reference component, ϕ_{PS} is the volume fraction of PS in a PS/PEB blend, and T is the absolute temperature. Equation 18 was obtained from cloud point measurements for PS/PEB pairs with varying 1-butene content[36] and by varying χ to produce the best fit, with the aid of the Flory−Huggins theory,[49,50] to the experimental temperature−composition phase diagram. A summary of predicted T_{ODT} is given in Table 10. It should be mentioned that eq 18 was obtained for fairly low molecular weights of PS and PEB, namely, M_w = 1500 for PS and M_w = 3880 for PEB with 84% 1-butene.

In view of the fact that α may depend on the molecular weight of the constituent components, the estimated T_{ODT}'s given in Table 10 may be regarded as being very conservative values, because the molecular weights of the SEB and SEBS block copolymers employed by various research groups[3,4] are far greater than those used to obtain eq 18. In Table 10 we observe that predicted T_{ODT}'s are much higher than the melt blending temperatures employed (say 300 °C as the highest value). This observation suggests that the SEB and SEBS block copolymers employed by various research groups[3,4] could not have formed an interphase during melt blending and thus could not have played the role of an effective compatibilizing agent. However, such block copolymers might have played the role of emulsifying agent to reduce the domain size.

An emulsifying agent reduces the interfacial tension between two immiscible liquids without necessarily forming an interphase, and thus it will not significantly improve mechanical properties of two immiscible homopolymers. On the other hand, an effective compatibilizing agent is expected to significantly improve the mechanical properties of an immiscible blend by forming an "interphase". Thus, emulsifying agent is *not* synonymous with compatibilizing agent.

It is appropriate to mention, at this juncture, the reason that the Helfand−Wasserman theory, together with eq 18, was used to estimate the T_{ODT}'s of SEB and SEBS block copolymers, whereas the Leibler theory, together with eq 17, was used to estimate T_{ODT}'s of PS-*block*-PMMA copolymers. As amply demonstrated in the literature,[51,52] the temperature dependence of the interaction parameter (χ or α) determined from cloud point measurements for an A/B binary blend turns out to be different from that determined from radiation scattering experiments for an A-*block*-B copolymer. Specifically, the coefficient B determined from radiation scattering methods in the expression χ (or α) $= A + B/T$ has been found to be smaller than that determined from cloud point measurement.[51] The T_{ODT} of block copolymer predicted from the Leibler theory, together with the temperature-dependent χ expression obtained from radiation scattering, has been found to agree reasonably well with experimental results. This is not surprising, because the Leibler theory was used to determine the temperature-dependent χ expression when radiation scattering methods were used. However, it has been observed[51] that the T_{ODT} of block copolymer predicted from the Leibler theory, together with the temperature-dependent χ expression obtained from cloud point measurement, was much higher (say ca. 60−100 °C) than experimental results. This is especially the case for symmetric or nearly symmetric block copolymers, whereas the agreement between prediction and experiment was reasonably good when the Helfand−Wasserman theory, together with the temperature-dependent χ expression obtained from cloud point measurements, was used. On the other hand, the T_{ODT} of block copolymer predicted from the Helfand−Wasserman theory, together with the temperature-dependent χ expression obtained from radiation scattering, has been found to be much lower than experimental results.[51] For this reason, above we have used the Leibler theory, together with eq 17, to predict T_{ODT}'s of PS-*block*-PMMA copolymers and the Helfand−Wasserman theory, together with eq 18, to predict T_{ODT}'s of SEB and SEBS block copolymers. Very recently, on the basis of cloud point measurements for a pair of homopolymers, poly(ethylene) (PE) and poly(ethylene propylene) (PEP), and small-angle neutron scattering experiments for a series of PE-*block*-PEP copolymers, Maurer et al.[52] concluded that the Leibler theory[46] and the fluctuation-corrected version[53] failed to reproduce the homopolymer result in obtaining temperature-dependent χ expression and that a more comprehensive block copolymer theory, which can accommodate chain polarization and stretching in the vicinity of the order−disorder transition, was needed.

It should be mentioned that melt blending of a pair of immiscible homopolymers with a block copolymer in a static mixing device (e.g., Mini-Max mixer, Brabender Plasticorder) for 5 min, for instance, would not yield an equilibrium morphology, because 5 min of mixing is too short to achieve an equilibrium morphology. Needless to say, the situation would depend very much on the molecular weight of polymers to be melt blended and melt blending temperature, which in turn controls the viscosities of the polymers. The higher the viscosities of the polymers to be melt blended, the slower will be the rate of polymer−polymer interdiffusion and thus the longer mixing time will be required to achieve an equilibrium morphology. The same argument would also be true for melt blending in an extruder, because the typical residence time in an extruder would be shorter than 5 min. On the other hand, as amply demonstrated above, the rate of formation of an interphase during melt blending of two immiscible homopolymers with a block copolymer in a given mixing device would also depend on two other important factors: (i) the extent of attractive thermodynamic interactions between a homopolymer and the corresponding block of copolymer and (ii) melt blending temperature in relation to the T_{ODT} of block copolymer.

Using the random phase approximation (RPA) theory, some research groups[54−56] regarded a block copolymer as being an effective compatibilizing agent when it satisfies the inequality $\partial(\chi N)_{s,macro}/\partial\phi_1 > 0$, where subscript s,macro denotes spinodal condition for macrophase separation transition, N is degree of polymerization, and ϕ_1 is the volume fraction of the block copolymer in a ternary blend consisting of two immiscible homopolymers and a block copolymer. Kim[56] appropriately cautioned that such a criterion based on the RPA theory may not be valid for a pair of highly immiscible homopolymers. Within the context of the requirements delineated in this paper, namely, attractive thermodynamic interactions must exist between a homopolymer and the corresponding block of copolymer and the T_{ODT} of block copolymer must be lower than the intended melt blending temperature, in order for a block copolymer to be an effective compatibilizing agent, $\partial(\chi N)_{s,macro}/\partial\phi_1 > 0$ cannot be regarded as being a useful criterion for the compatibilization of two immiscible homopolymers.

Using the self-consistent mean-field approach, some research groups[57−60] developed expressions enabling one to calculate the interfacial tension between two immiscible homopolymers in the presence of a block copolymer. The rationale behind such calculations lies in the notion that an effective compatibilizing agent would decrease the interfacial tension between two immiscible homopolymers. As pointed out above, lowering the interfacial tension of immiscible polymer blend alone is *not* sufficient for one to claim that a block copolymer functions as an effective compatibilizing

agent *unless* an 'interphase' is formed in which a homopolymer and the corresponding block of copolymer coexist (see Figure 1).

Concluding Remarks

In this paper we have demonstrated that two requirements must be met if a block copolymer is going to be an effective compatibilizing agent for two immiscible homopolymers. They are (i) attractive thermodynamic interactions between a homopolymer and the corresponding block of copolymer must be present and (ii) block copolymer must be designed such that its T_{ODT} is lower than the intended melt blending temperature.

One cannot expect to have an "interphase" formed, during melt blending, between a homopolymer and the corresponding block of copolymer unless they have attractive thermodynamic interactions. In this study we have shown, via TEM, the formation of an interphase in (i) PS/PB/(PαMS-*block*-PI) (see Figure 5) and (ii) PPO/PP/(PS-*block*-PEB) (see Figure 12) model ternary blends. Such experimental observations are supported by the attractive thermodynamic interactions (negative χ) existing (i) between homopolymer PB (with high 1,2-addition) and PI block of PαMS-*block*-PI copolymer and (ii) between homopolymer PPO and PS block of PS-*block*-PEB copolymer and between homopolymer PP and PEB block (with high 1-butene content) of PS-*block*-PEB copolymer. On the other hand, we did not observe the formation of an interphase in PMMA/PP/(PαMS-*block*-PI) ternary blend (Figure 16), which was explained by the fact that only repulsive interactions exist in any pairs of component polymers.

We have demonstrated further that even when attractive thermodynamic interactions exist between a homopolymer and the corresponding block of copolymer, no interphase was formed when the melt blending temperature employed was lower than the T_{ODT} of block copolymer (Figures 8a and 14a). The absence of an interphase under such circumstances is attributed to the very high viscosity of the microphase-separated block copolymers. The readers are reminded that the viscosity of a block copolymer in an ordered state (i.e., at $T < T_{ODT}$) is 2−4 orders of magnitude higher than that in the disordered state (i.e., at $T > T_{ODT}$) and that melt blending times in practical polymer processing operations (e.g., in an extruder) would not exceed 5 min. In this regard, it is fair to state that an equilibrium morphology in a ternary blend consisting of two homopolymers and a block copolymer cannot be expected during practical melt blending operations.

Because of the lack of a sufficient quantity of model block copolymers synthesized in this study, the mechanical properties of ternary blends prepared could not be tested. However, it is not difficult to surmise that no significant improvement in mechanical properties of ternary blends is expected if no "interphase" of a sufficient thickness is formed by addition of a block copolymer to two immiscible homopolymers. It should be emphasized that the primary objective of the present study was to test the concept advanced in our previous study.[29] Having demonstrated that the concept is valid, in the future we will conduct further experiments including measurements of mechanical properties and adhesion of A/B/(C-*block*-D) ternary blends by synthesizing larger quantities of model block copolymers.

At present we do not have a comprehensive theory enabling one to predict, during melt processing, the "width of interphase" in A/B/(C-*block*-D) ternary blends as functions of the molecular weights of two homopolymers A and B, the molecular weight and block length ratio of C-*block*-D copolymer, blend composition, and the interaction parameters that in turn depend on temperature. When such a theory is developed, A/B/(A-*block*-B), A/B/(A-*block*-D), and A/B/(C-*block*-B) ternary systems can be treated as a special case of the A/B/(C-*block*-D) ternary system. Further, when such a theory becomes available, one can minimize very time-consuming and costly, sometimes unnecessary, experiments. We are not aware of any work in the literature reporting on all six pairs of temperature-dependent interaction parameters associated with A/B/(C-*block*-D) ternary blends investigated in this study (Table 4). Such information will be very valuable to assess the validity of theory. The experimental results presented in this paper will be useful to stimulate future theoretical development predicting the effectiveness of C-*block*-D copolymer as a compatibilizing agent for two immiscible homopolymers A and B.

Before closing, we would like to point out that the molecular weight of each component plays an important role in the rate of formation of an *interphase*. Specifically, a block copolymer will act as an *effective* compatibilizing agent only when the molecular weights of block chains and the corresponding homopolymer lie within a certain range, because the rate of interdiffusion between the components depends on molecular weight. The molecular viscoelasticity theory[62] suggests that the center-of-mass diffusion coefficient (D_o) of a polymer is inversely proportional to molecular weight M (i.e., $D_o \sim 1/M$) for $M < M_c$ and $D_o \sim 1/M^2$ for $M > M_c$, where M_c is the critical molecular weight for entanglement. This means that when $M > M_c$ the interdiffusion would be very slow. From the point of view of mechanical properties, it is highly desirable to have $M > M_c$ so that the chains would not be easily pulled out from the interphase when an external force is applied. However, as amply demonstrated in this paper, the molecular weights of block chains and the corresponding homopolymer must lie within a certain range if the block copolymer is going to act as an *effective* compatibilizing agent. Therefore, it is very important for one to determine an optimum range of molecular weights in the design of block copolymers for compatibilizing agent.

Acknowledgment. We acknowledge with gratitude that Dr. Adel Halasa of Goodyear Tire and Rubber Company supplied us with PB-12, PB-80, PI-200, SB-17, and SB diblock copolymers which were used to obtain, via hydrogenation, SEB-15 and SEB-19 and that Dr. Norberto Silvi of General Electric Company supplied us with PPO employed in this study.

Appendix

When we prepared χ versus $1/T$ plots using all 10 sets of data in Table 3 of ref 37, we found the following anomalies: (i) the data set for the PI($x = 0.07$)/PB($y = 0.09$) with $\phi_A(0.52)/\phi_B(0.48)$ gave an unusually high slope, (ii) the data set for the PI($x = 0.07$)/PB($y = 0.26$) with $\phi_A(0.52)/\phi_B(0.48)$ gave an unusually high slope, and (iii) two data sets for the PI($x = 0.07$))/PB($y = 0.39$) with $\phi_A(0.52)/\phi_B(0.48)$ and $\phi_A(0.32)/\phi_B(0.68)$ showed inconsistency, compared to other data sets, in that a regular microstructure dependence could not be observed. Further, we found that (i) the predicted plots of χ versus

$1/T$, via eqs 10 of ref 37, produced a very poor correlation when using the following data set: (i) PI($x = 0.07$)/PB($y = 0.09$), (ii) PI($x = 0.21$)/PB($y = 0.70$), and (iii) PI($x = 0.44$)/PB($y = 0.70$). Therefore, from the total 10 sets of data in Table 3 of ref 37 we deleted the following four sets of data: (i) PI($x = 0.07$)/PB($y = 0.09$) with $\phi_A(0.52)/\phi_B(0.48)$, (ii) PI($x = 0.07$)/PB($y = 0.26$) with $\phi_A(0.52)/\phi_B(0.48)$, (iii) PI($x = 0.07$))/PB($y = 0.39$) with $\phi_A(0.52)/\phi_B(0.48)$, and (iv) PI($x = 0.07$)/PB($y = 0.39$) with $\phi_A(0.32)/\phi_B(0.68)$ and then curve-fitted the rest of the data set to the following expression (eq 10 in ref 37):

$$\chi(x,y) = xy\chi_1 + (1-x)y\chi_2 + x(1-y)\chi_3 + (1-x)(1-y)\chi_4 - x(1-x)\chi_5 - y(1-y)\chi_6 \quad \text{(A1)}$$

with

$$\chi_i = a_i + b_i/T + c_i\phi_B/T \quad (i = 1, 2\ 3, 4, 5, 6) \quad \text{(A2)}$$

where x is the volume fraction of 3,4-addition in PI, y is the volume fraction of 1,2-addition in PB, χ_i are the Flory−Huggins interaction parameters with a_i, b_i, and c_i being curve-fitting parameters, ϕ_B is the volume fraction of PB in a PB/PI blend, and T is the absolute temperature. In other words, 18 coefficients—a_i ($i = 1$, 2, 3, 4, 5, 6), b_i ($i = 1$, 2, 3, 4, 5, 6), and c_i ($i = 1$, 2, 3, 4, 5, 6)—were determined by minimizing the difference between the measured and calculated values of $\chi(x,y)$ by use of the multivariable regression analysis. The computed expressions for six χ_i are given below.

$$\chi_1 = 6.83 \times 10^{-3} - 15.1/T + 6.42\phi_{PB}/T \quad \text{(A3)}$$

$$\chi_2 = 1.16 \times 10^{-2} - 5.15/T - 0.38\phi_{PB}/T \quad \text{(A4)}$$

$$\chi_3 = 3.67 \times 10^{-2} - 6.77/T - 4.23\phi_{PB}/T \quad \text{(A5)}$$

$$\chi_4 = 2.30 \times 10^{-3} - 2.72/T + 1.93\phi_{PB}/T \quad \text{(A6)}$$

$$\chi_5 = 2.72 \times 10^{-2} - 17.0/T + 3.33\phi_{PB}/T \quad \text{(A7)}$$

$$\chi_6 = 1.31 \times 10^{-2} - 7.61/T + 1.47\phi_{PB}/T \quad \text{(A8)}$$

We found that eq A1 together with eqs A3−A8 reproduced Figures 4 and 7 given in ref 37.

We would like to comment on the choice of eq A2 in place of eq 9 (involving four coefficients) of ref 37. Note that the Gibbs free energy change ΔG_M accompanying the mixing of component A of molar volume V_A with component B of molar volume V_B, evaluated for unit volume of the mixture, is given by[61]

$$\Delta G_M = RT[(1/V_A)\phi_A \ln \phi_A + (1/V_B)\phi_B \ln \phi_B] + \Lambda\phi_A\phi_B \quad \text{(A9)}$$

where R is the universal gas constant, T is the absolute temperature, ϕ_A and ϕ_B are the volume fractions of the components, and Λ can be regarded as the polymer−polymer interaction parameter representing all the free energy of mixing that is not accounted for by the combinatory entropy of mixing (i.e., the first term on the right-hand side of eq A9). On the basis of their experimental data, Roe and Zin[61] expressed Λ in terms of composition ϕ_B and temperature T by

$$\Lambda = \lambda_o + \lambda_1\phi_B + \lambda_T T \quad \text{(A10)}$$

where λ_o, λ_1, and λ_T are curve-fitting parameters. They noted further that when Λ and χ do not depend on the composition, Λ is related to χ by

$$\chi = V_r\Lambda/RT \quad \text{(A11)}$$

with V_r being the molar volume of reference component. It can now be seen that eq A2 can be obtained from eqs A10 and A11, suggesting that eq A2 has a thermodynamic origin.

For the 63/27/10 PS/PB/(PαMS-*block*-PI) ternary blend employed in our experiment, homopolymer PB has 91% 1,2-addition and PI block has 59% 3,4-addition. Thus, substituting $x = 0.59$ and $y = 0.91$ into eq A1, with the aid of eqs A3−A8, we obtain eq 6 in Table 4.

References and Notes

(1) Löwenhaupt, B.; Hellmann, G. P. *Colloid Polym. Sci.* **1990**, *268*, 885.

(2) Adedeji, A.; Jamieson, A. M.; Hudson, S. D. *Macromol. Chem. Phys.* **1996**, *197*, 2521.

(3) (a) Fayt, R.; Jérôme, R.; Teyssie, Ph. *J. Polym. Sci., Polym. Lett. Ed.* **1981**, *19*, 79. (b) Fayt, R.; Jérôme, R.; Teyssie, Ph. *J. Polym. Sci., Polym. Phys. Ed.* **1982**, *20*, 2209. (c) Fayt, R.; Jérôme, R.; Teyssie, Ph. *Makromol. Chem.* **1986**, *187*, 837. (d) Fayt, R.; Jérôme, R.; Teyssie, Ph. *J. Polym. Sci., Polym. Phys. Ed.* **1986**, *24*, 25. (e) Fayt, R.; Jérôme, R.; Teyssie, Ph. *Polym. Eng. Sci.* **1987**, *27*, 328. (f) Fayt, R.; Jérôme, R.; Teyssie, Ph. *J. Polym. Sci., Polym. Phys. Ed.* **1989**, *27*, 775. (g) Harrats, C.; Blacher, S.; Fayt, R.; Jérôme, R.; Teyssie, Ph. *J. Polym. Sci., Polym. Phys. Ed.* **1995**, *33*, 801.

(4) (a) Traugott, T. D.; Barlow, J. W.; Paul, D. R. *J. Appl. Polym. Sci.* **1983**, *28*, 2947. (b) Barlow, J. W.; Paul, D. R. *Polym. Eng. Sci.* **1984**, *24*, 525. (c) Schwarz, M. C.; Barlow, J. W.; Paul. D. R. *J. Appl. Polym. Sci.* **1988**, *35*, 2053. (d) Schwarz, M. C.; Barlow, J. W.; Paul. D. R. *J. Appl. Polym. Sci.* **1989**, *37*, 403. (e) Park, I.; Barlow, J. W.; Paul, D. R. *J. Appl. Polym. Sci.* **1992**, *45*, 1313. (f) Gupta, A. K.; Purwar, S. N. *J. Appl. Polym. Sci.* **1985**, *30*, 1799. (g) Setz, S.; Stricker, F.; Kressler, J.; Duschek, T.; Mülhaupt, R. *J. Appl. Polym. Sci.* **1996**, *59*, 1117. (h) Heck, B.; Arends, P.; Ganter, M.; Kressler, J.; Stühn, B. *Macromolecules* **1997**, *30*, 4559.

(5) Ouhadi, T.; Fayt, R.; Jérôme, R.; Teyssie, Ph. *J. Polym. Sci., Polym. Phys. Ed.* **1986**, *24*, 973.

(6) Fayt, R.; Teyssie, Ph. *Polym. Eng. Sci.* **1989**, *29*, 538.

(7) Jo, W. H.; Kim, H. C.; Baek, D. H. *Macromolecules* **1991**, *24*, 2231.

(8) Kim, H. C.; Nam, K. H.; Jo, W. H. *Polymer* **1993**, *34*, 4043.

(9) Jo, W. H.; Jo, B. C.; Cho, J. C. *J. Polym. Sci., Polym. Phys. Ed.* **1994**, *32*, 1661.

(10) Auschra, C.; Stadler, R.; Voigt-Martin, I. G. *Polymer* **1993**, *34*, 2081.

(11) Auschra, C.; Stadler, R.; Voigt-Martin, I. G. *Polymer* **1993**, *34*, 2094.

(12) Kim, J. R.; Jamieson, A. M.; Hudson, S.; Manas-Zloczower, I.; Ishida, H. *Macromolecules* **1998**, *31*, 5383.

(13) Majumdar, B.; Paul, D. R.; Oshinski, A. J. *Polymer* **1997**, *38*, 1787.

(14) Kim, S.; Kim, J. K.; Park, C. E. *Polymer* **1997**, *38*, 1809, 2113, 2115.

(15) Jeon, H. K.; Kim, J. K.; Park, C. E. *Macromolecules* **1998**, *31*, 9273.

(16) Wildes, G. S.; Harada, T.; Keskkula, H.; Paul, D. R.; Janarthanan, V.; Padwa, A. R. *Polymer* **1999**, *40*, 3069.

(17) Champagne, M. F.; Huneault, M. A.; Roux, C.; Peyrel. W. *Polym. Eng. Sci.* **1999**, *39*, 976.

(18) Shull, K. R.; Kramer, E. J.; Hadziioannou, G.; Tang, W. *Macromolecules* **1990**, *23*, 4780.

(19) Russell, T. P.; Menelle, A.; Hamilton, W. A.; Smith, G. S.; Satija, S. K.; Majkrzak, C. F. *Macromolecules* **1991**, *24*, 5721.

(20) Russell, T. P.; Anastasiadis, S.; Menelle, A.; Felcher,. P.; Satija, S. K. *Macromolecules* **1991**, *24*, 1575.

(21) Dai, K. H.; Kramer, E. J.; Shull, K. R. *Macromolecules* **1992**, *25*, 220.

(22) (a) Brown, H. R.; Char, K.; Deline. V. R.; Green, P. F. *Macromolecules* **1993**, *26*, 4155. (b) Char, K.; Brown, H. R.; Deline. V. R. *Macromolecules* **1993**, *26*, 4164. (c) Reichert, W. F.; Brown, H. R. *Polymer* **1993**, *34*, 2291. (d) Creton, C.; Kramer, E. J.; Hui, C. Y.; Brown, H. R. *Macromolecules* **1992**, *25*, 3075.
(23) Edgecombe, B. D.; Stein, J. A.; Frechet, M. J.; Xu, Z.; Kramer, E. J. *Macromolecules* **1998**, *31*, 1292.
(24) Noolandi, J.; Hong, K. M. *Macromolecules* **1982**, *15*, 482.
(25) Shull, K. R.; Kramer, E. J. *Macromolecules* **1990**, *23*, 4769.
(26) Banaszak, M.; Whitmore, M. D. *Macromolecules* **1992**, *25*, 249, 2757.
(27) Janert, P. K.; Schick, M. *Macromolecules* **1997**, *30*, 137.
(28) Vilgis, T. A.; Noolandi, J. *Macromolecules* **1990**, *23*, 2941.
(29) Chun, S. B.; Han, C. D. *Macromolecules* **1999**, *32*, 4030.
(30) Morese-Seguela, B.; St-Jaques, M.; Renaud, J. M.; Prud'homme, J. *Macromolecules* **1980**, *13*, 100.
(31) Han, C. D.; Baek, D. M.; Kim, J. K. *Macromolecules* **1995**, *28*, 5886.
(32) Hahn, S. F. *J. Polym. Sci., Polym. Chem. Ed.* **1992**, *30*, 397.
(33) Kim, J. K. Molecular Aspects of Viscoelasticity for Compatible Polymer Blends and Block Copolymers. Doctoral Dissertation, Polytechnic University, Brooklyn, NY, 1990.
(34) (a) Gouinlock, E. V.; Porter, R. S. *Polym. Eng. Sci.* **1977**, *17*, 535. (b) Chung, C. I.; Lin, M. I. *J. Polym. Sci., Polym. Phys. Ed.* **1978**, *16*, 545. (c) Widmaier, J. M.; Meyer, G. C. *J. Polym. Sci., Polym. Phys. Ed.* **1980**, *18*, 2217.
(35) Lin, J. L.; Roe, R.-J. *Macromolecules* **1987**, *20*, 2168.
(36) Han, C. D.; Chun, S. B.; Hahn, F. S.; Harper, S. Q.; Savickas, P. J.; Meunier, D. J.; Li, L.; Yalcin, T. *Macromolecules* **1998**, *31*, 394.
(37) Thudium, R. N.; Han, C. C. *Macromolecules* **1996**, *29*, 2143.
(38) Maconnachie, A.; Kambour, R. P.; White, D. M.; Rostami, S.; Walsh, D. J. *Macromolecules* **1984**, *17*, 2645.
(39) ten Brinke, Karasz, F. E.; Macknight, W. J. *Macromolecules* **1983**, *16*, 1827.
(40) Graessley, W. W.; Krishnamoorti, R.; Reichert, G. C.; Balsara, N. P.; Fetters, L. J.; Lohse, D. J. *Macromolecules* **1995**, *28*, 1260.
(41) Jeon, H. S.; Lee, J. H.; Balsara, N. P.; Nestein, M. C. *Macromolecules* **1998**, *31*, 3340.
(42) Graessley, W. W.; Krishnamoorti, R.; Balsara, N. P.; Butera, R. J.; Fetters, L. J.; Lohse, D. J.; Schulz, D. N.; Sissano, J. A. *Macromolecules* **1994**, *27*, 3896.
(43) Fayt, R.; Jérôme, R.; Teyssie, Ph. *J. Polym. Sci., Polym. Chem. Ed.* **1989**, *27*, 2823.
(44) Macosko, C. W.; Guegan, P.; Khandpur, A. K.; Nakayama, A.; Marechal. P.; Inoue, T. *Macromolecules* **1996**, *29*, 5590.
(45) Adedeji, A.; Jamieson, A. M.; Hudson, S. D. *Macromol. Chem. Phys.* **1996**, *197*, 2521.
(46) Leibler, L. *Macromolecules* **1980**, *13*, 1602.
(47) Russell, T. P.; Hjelm, R. P.; Seeger, P. A. *Macromolecules* **1990**, *23*, 890.
(48) Helfand, E.; Wasserman, Z. R. In *Developments in Block Copolymers*; Goodman, I., Ed.; Applied Science: New York, 1982; Chapter 4.
(49) Flory, P. J. *J. Chem. Phys.* **1941**, *9*, 660; **1942**, *10*, 51; **1945**, *13*, 453.
(50) Huggins, M. L. *J. Chem. Phys.* **1941**, *9*, 440; *J. Phys. Chem.* **1942**, *46*, 151.
(51) Han, C. D.; Baek, D. M.; Kim, J. K.; Ogawa, T.; Sakamoto, N.; Hashimoto, T. *Macromolecules* **1995**, *28*, 5043.
(52) Maurer, W. W.; Bates, F. S.; Lodge, T. P.; Almdal, K.; Mortensen, K.; Fredrickson, G. H. *J. Chem. Phys.* **1998**, *108*, 2989.
(53) Fredrickson, G. H.; Helfand, E. *J. Chem. Phys.* **1987**, *87*, 697.
(54) Tanaka, H.; Hashimoto, T. *Polym. Commun.* **1988**, *29*, 212.
(55) Kim, J. K.; Kimishima, K.; Hashimoto, T. *Macromolecules* **1993**, *26*, 125.
(56) Kim, J. K. *Polymer* **1995**, *36*, 1243.
(57) Noolandi, J.; Hong, K. M. *Macromolecules* **1982**, *15*, 482.
(58) Leibler, L. *Macromol. Chem. Macromol. Symp.* **1988**, *16*, 1.
(59) Leibler, L. *Physica A* **1991**, *172*, 258.
(60) Noolandi, J. *Makromol. Chem. Rapid Commun.* **1991**, *12*, 517.
(61) Roe, R.-J.; Zin, W.-C. *Macromolecules* **1980**, *13*, 1221.
(62) Doi, M.; Edwards, S. F. *The Theory of Polymer Dynamics*; Clarendon Press: Oxford, 1986.

MA9918708